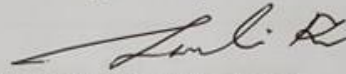


**Analysis of Micro-Strip Patch Sensor of Various  
Sizes and Parameters for Non-invasive  
Electrolyte Sensing**

Approved by



**Dr. Md. Taslim Reza**

**Supervisor and Professor  
Department of Electrical and Electronic Engineering (EEE)  
Islamic University of Technology (IUT)  
Gazipur-1704, Bangladesh**

Date: 18.05.2022

## Declaration of Authorship

This is to certify that the work presented in this thesis paper is the outcome of research carried out by the candidates under the supervision of Dr. Md. Taslim Reza, Professor, Department of Electrical and Electronic Engineering (EEE), Islamic University of Technology (IUT). It is also declared that neither this thesis paper nor any part thereof has been submitted anywhere else for the reward of any degree or any judgment.

### Authors

*Fardeen*

---

**Fardeen Md. Toushique**  
ID-170021137

*Saikot*

---

**Shoeb Mahmud Saikot**  
ID-170021035

*Talha*

---

**Talha Bin Nizam**  
ID-170021140

# **Analysis of Micro-Strip Patch Sensor of Various Sizes and Parameters for Non-invasive Electrolyte Sensing**

by

**Fardeen Md. Toushique (170021137)**

**Shoeb Mahmud Saikot (170021035)**

**Talha Bin Nizam (170021140)**

**A Thesis Submitted to the Academic Faculty in Partial Fulfillment of the Requirements for the Degree of**

**Bachelor of Science in Electrical and Electronic Engineering**



**Department of Electrical and Electronic Engineering**

**Islamic University of Technology (IUT)**

**Gazipur, Bangladesh**

**May, 2022**

# **Analysis of Micro-Strip Patch Sensor of Various Sizes and Parameters for Non-invasive Electrolyte Sensing**

Approved by

-----  
**Dr. Md. Taslim Reza**

**Supervisor and Professor  
Department of Electrical and Electronic Engineering (EEE)  
Islamic University of Technology (IUT)  
Gazipur-1704, Bangladesh**

Date:

## **Declaration of Authorship**

This is to certify that the work presented in this thesis paper is the outcome of research carried out by the candidates under the supervision of Dr. Md. Taslim Reza, Professor, Department of Electrical and Electronic Engineering (EEE), Islamic University of Technology (IUT). It is also declared that neither this thesis paper nor any part thereof has been submitted anywhere else for the reward of any degree or any judgment.

### **Authors**

-----  
**Fardeen Md.Toushique**  
ID-170021137

-----  
**Shoeb Mahmud Saikot**  
ID-170021035

-----  
**Talha Bin Nizam**  
ID-170021140

*Dedicated*

*to*

*Our beloved parents, whose support made  
it all possible for us*

# TABLE OF CONTENTS

## Chapter 1

### Introduction

1.1 Introduction.....	2-3
1.2 Significance of the Research.....	3-4
1.3 Objectives of this Research.....	5
1.4 Thesis Outline.....	5

## Chapter 2

### Literature Review

2.1 Introduction to Micro-Strip Patch antenna.....	6-7
2.2 Use of Micro-Strip Patch Antenna in Biomedical applications.....	7-8
2.2.1 Breast Cancer Detection.....	7
2.2.2 Telemedicine and Electromagnetic Imaging Techniques.....	7
2.2.3 Medical Implant Communications Service.....	7
2.2.4 Micro-strip Patch Antenna For Health Care Monitoring.....	8
2.3 Various Electrolyte Measuring Techniques.....	8-11
2.3.1 Ion-Selective Electrode.....	8-9
2.3.2 Energy-Resolved Optical Non-invasive Electrolyte Detection.....	9
2.3.3 NaLiK for Electrolyte Detection.....	10
2.3.4 Integrated Ion-selective Optode Sensor Cartridge for Direct Electrolyte Detection... ..	10
2.3.5 Non-invasive Micro-Strip Patch Sensor for Electrolyte Detection.....	11
2.4 Non-Invasive Measurement Techniques.....	11-13
2.4.1 Non-invasive Measurement of Blood Components.....	11

2.4.2 Techniques for Non-Invasive Monitoring of Arterial Blood Pressure.....	11-12
2.4.3 Non-Invasive Measurements in the Assessment of Bladder Outlet Obstruction.....	12
2.4.4 Non-invasive spectroscopic techniques in the diagnosis of non-melanoma skin cancer	12
2.4.5 Non-invasive measurements of carboxyhemoglobin and methemoglobin in children with sickle cell disease	
2.5 Sensor Classification.....	13-16
2.5.1 Electrochemical Sensors.....	13-14
2.5.2 Potentiometric Sensors.....	14
2.5.3 Amperometric Sensors.....	14-15
2.5.4 Coulometric.....	15
2.5.5 Conductometric Sensors.....	16
2.6 Sensor Characteristics.....	16-18
2.6.1 Sensor Sensitivity.....	16-17
2.6.2 Sensor Linearity.....	17-18
2.6.3 Error.....	18-19
Systematic Error.....	18
Random Error.....	19

## **Chapter 3**

### **Methodology**

3.1 Introduction.....	
3.2 Reference design.....	20
3.3 Electrolyte solution concentration.....	20-21
3.4 Change of antenna parameters.....	21-22
3.5 Sensitivity comparison.....	22
3.6 Linearity comparison.....	23



3.7 Error comparison.....	23
---------------------------	----

## **Chapter 4**

### **Results and Discussion**

4.1 Total size variation of MPA-based sensor.....	24-37
4.1.1 Sensitivity.....	24-26
4.1.2 Linearity.....	27-36
4.1.3 Error Calculation.....	37
4.2 Feed line width variation of MPA-based sensor.....	38-51
4.2.1 Sensitivity.....	38-40
4.2.2 Linearity.....	41-50
4.2.3 Error Calculation.....	51
4.3 Discussion.....	52

## **Chapter 5**

### **Future Goals and Conclusion**

5.1 Introduction.....	53
5.2 Future goals.....	53
5.3 Conclusion.....	53
References.....	54-58

## LIST OF FIGURES

Figure No.	Name of the Figure	Page No.
2.1	Basic Structure of a micro-strip patch antenna	8
2.2	Wearable sensor for remote healthcare monitoring system	10
2.3	Sensor Sensitivity	12
2.4	Sensor Linearity	14
3.1	Flowchart	
3.2	Micro-strip Patch antenna design	16
4.1	Resonant frequency vs NaCl concentration curve for five Different MPA-based sensor size	17
4.2	Reflection co-efficient( $S_{11}$ ) vs NaCl concentration curve for five different MPA-based sensor size	19
4.3	Frequency Vs Concentration for 20% decrease antenna size	20
4.4	Frequency Vs Concentration for 10% decrease	23
4.5	Frequency Vs Concentration for actual antenna size	25
4.6	Frequency Vs Concentration for 10% increase antenna size	26
4.7	Frequency Vs Concentration for 20% increase antenna size	28
4.8	$S_{11}$ Vs NaCl concentration 20% decrease antenna size	30
4.9	$S_{11}$ Vs NaCl concentration 10% decrease antenna size	31
4.10	$S_{11}$ Vs NaCl concentration actual antenna size	37
4.11	Frequency Vs Concentration for 10% increase antenna size	41
4.12	Frequency Vs Concentration for 20% increase antenna size	45
4.13	$S_{11}$ Vs Resonant frequency plot for five different MPA-based sensor size having NaCl Concentration 0.062 mol/L	47
4.14	Resonant frequency vs NaCl concentration curve for five different MPA-based sensor size by varying feed line.	50
4.15	Reflection co-efficient ( $S_{11}$ ) vs NaCl concentration curve for five different MPA-based sensor sizes by varying feed line	53
4.16	Frequency Vs Concentration for 20% decrease antenna size by varying feed-line	53
4.17	Frequency Vs Concentration for 10% decrease antenna size by varying feed-line	54

4.18	Frequency Vs Concentration for actual antenna size by varying feed-line	55
4.19	Frequency Vs Concentration for 10% increase antenna size by varying feed-line	57
4.20	Frequency Vs Concentration for 20% increase antenna size by varying feed-line	57
4.21	$S_{11}$ Vs Concentration for 20% decrease antenna size by varying feed-line	58
4.22	$S_{11}$ Vs Concentration for 10% decrease antenna size by varying feed-line	58
4.23	$S_{11}$ Vs Concentration for actual antenna size by varying feed-line	59
4.24	$S_{11}$ Vs Concentration for 10% increase antenna size by varying feed-line	60
4.25	$S_{11}$ Vs Concentration for 20% increase antenna size by varying feed-line	61
4.26	$S_{11}$ Vs Resonant frequency plot for five different MPA-based sensor size by varying feed-line and having NaCl Concentration 0.062 mol/L	62

## LIST OF TABLES

<b>Table No.</b>	<b>Name of the Table</b>	<b>Page No.</b>
3.1	Dielectric Parameters of NaCl Concentrations at 20°C	3
3.2	Changed antenna parameters	52
3.3	Changed antenna feed-line width parameters	55
4.1	Sensitivity Table (Total size variation)	56
4.2	Error chart for 0.062 mol/L concentration of NaCl Solution (Total size variation)	56
4.3	Sensitivity Table (Feed line width variation)	59
4.4	Error chart for 0.062 mol/L concentration of NaCl solution (Feed-line width variation)	60

## **LIST OF ABBREVIATIONS**

<b>MPA</b>	Micro-Strip Patch Antenna
<b>ISE</b>	Ion Selective Electrodes
<b>AAS</b>	Atomic Absorption Spectroscopy
<b>ECG</b>	Electrocardiogram
<b>PCB</b>	Printed Circuit Board
<b>MBI</b>	Microwave Breast Imaging
<b>ISM</b>	Industrial Scientific and Medical bands
<b>MICS</b>	Medical Implant Communication Service
<b>CPW</b>	Coplanar Waveguide
<b>VWSR</b>	Voltage Wave Standing Ratio
<b>CKD</b>	Chronic Kidney Disease
<b>OES</b>	Optical Emission Spectroscopy
<b>BP</b>	Blood Vessel Pulse
<b>LUTS</b>	Lower Urinary Lot Side
<b>BOO</b>	Blood Outlet Obstruction
<b>SCD</b>	Sickle Cell Disease
<b>DC</b>	Direct Current
<b>IC</b>	Integrated Circuit
<b>SNR</b>	Signal to Noise Ratio

## ACKNOWLEDGEMENTS

We would like to express her heartiest sense of gratitude to the “Almighty Allah” Who has enabled us to complete the dissertation works successfully.

We express our heartfelt gratitude, sincere regards to our thesis supervisor **Dr. Md. Taslim Reza** Sir whose support, motivation, patience, enthusiasm and extensive knowledge of the relevant fields has made it possible for us to complete this work. From day one sir motivated and inspired us. It is through his relentless efforts and dedication we are here today. Sir believed in our skills and did his best to guide us through this difficult journey. For this we will be eternally grateful.

We would also like to acknowledge and show our gratitude to the respected faculty member of Islamic University of Technology whose brilliant minds spent the better part of the last 4 years trying to enlighten us. They have not only positively affected our academic lives but also inspired us in our personal life.

We would also like to take this opportunity to thank all the members of IUT administration, staff, lab assistants and all the members of the IUT family whose tireless dedication to their works that has made the last 4 years in IUT a memorable event for us.

We would also like to express our heartfelt gratitude to our dear batchmates, juniors and seniors who have helped us in every step of the way and blessed us with their knowledge and companionship. All of them have truly inspired us to an extent that is unimaginable.

And finally we would like to express our utmost gratitude to the people closest to us our dear parents. They have sacrificed tirelessly for our sake. It is through their love and blessings that we have reached this milestone.

## **Abstract**

Electrolyte imbalance is a major health issue that can go unnoticed due to the lack of frequent testing. Most prevalent electrolyte monitoring measures require direct blood testing which is invasive in nature. Invasive monitoring measures are not only painful but also time-consuming. So non-invasive electrolyte monitoring is slowly gaining popularity. In this paper, non-invasive micro-strip patch antennas of different sizes and parameters have been analyzed. Micro-strip patch antennas of five different sizes and five different parameters have been analyzed for their sensitivity, linearity, and accuracy for a frequency range of 0.01GHz to 0.2GHz. Seven different concentrations of NaCl have been used for this analysis. Various research papers have found that there is a correlation between changing concentrations of NaCl and reflection coefficient  $S_{11}$  and resonant frequency. From this analysis, it has been observed that changing antenna size causes changes in antenna characteristics.

# Chapter 1

## Introduction

### 1.1 Introduction

In present world, electrolyte measurement has become much popular to monitor health condition by health personals and specialists. In medical science, electrolyte monitoring means collection & analysis of patient data to regulate electrolyte balance. It can be used for pulse rate check, heart beat monitor, daily exercise track. Most commonly used two techniques are-Blood detection & Sweat detection. In our study, we'll use sweat detection technique for electrolyte measurement. To detect electrolyte concentration from human sweat we have proposed micro-strip patch antennas that can detect electrolyte concentration by utilizing antenna's electromagnetic properties. As we will be using sweat as our solution for electrolyte measurement it will be a non-invasive electrolyte measurement system. A non-invasive electrolyte measurement system doesn't harm other body parts or organs which is vitally important for the implementation of an electrolyte sensor that can be used frequently by most people. Along with the implementation of a sensor that can detect electrolytes non-invasively there is also the need to consider various factors such as their range of operation, sensitivity, linearity, error etc. To determine the design of an optimum micro-strip patch antenna that can operate under desired conditions we have done a comparative analysis of antennas with same design but different sizes. We have also done a comparative analysis by only changing one parameter of the antennas to see what changes occur in their characteristics. We compared these antennas for their sensitivity, linearity and error and tried to see which size gives the best result for which case. We have also tried to uncover if there are any patterns to how changing antenna sizes bring changes in their characteristics. The goal of all these analysis is to build a set of rules regarding the manipulation of antenna dimensions and how these manipulations effect their different parameters so that antenna manufacturers can use them to make antennas based on their requirements. The research will focus on electrolyte's effect on the dielectric material of the antenna and how these effects will manifest themselves in a change in the antennas electromagnetic properties. The entire research was done with a combination of software based simulation and mathematical analysis. COMSOL multiphysics software was used



for the simulation of the antennas, Matlab was used for generating the graphs and calculating the sensitivities and Excel was used to analyze the linearity of the antennas.

## **1.2 Significance of the Research**

Electrolyte imbalance is a life-threatening condition that needs immediate detection and treatment. Hypokalemia (low serum potassium) is the most common electrolyte anomaly, which arises as a result of potassium losses caused by self-induced vomiting or the use of diuretics or laxatives. There is Hyponatremia that arises from drinking too much water. Hypophosphatemia (low serum phosphorus) and hypomagnesemia (low serum magnesium) which causes multiple organ failures [1]. Electrolyte imbalances are all too common in emergency room and intensive care unit patients [2]. That's why the need for a fast, reliable and inexpensive electrolyte sensor arises. Generally clinical chemistry laboratories have very few methods for measuring electrolytes such as Na<sup>+</sup> and K<sup>+</sup>. The traditional procedures for assessing critical ion levels in plasma or other biological fluids are ion-selective electrodes (ISEs), flame photometry, and atomic absorption spectrometry (AAS) [3-6]. Even though ISEs, AAS and flame photometry are widely used, they are costly, immobile requires chemical reagents and expert operators [7-9]. Also some of these procedures require blood sample extracting which are not only painful but also may result in many health complications [10]. So that's why the need for non-invasive method of electrolyte detection arises which is low-cost, mobile and easy to manufacture [11]. There's a noticeable increase in the interest of health advice that uses non-invasive or minimally invasive wearable gadgets. Beyond physical markers, metabolic markers such as sweat or saliva provide a more visible display of human health, allowing us to make an accurate clinical diagnosis, measure a patient's blood sugar and blood pressure, perform athletics and guide chronic health situations, including raising emergency alerts [12]. Sweat is one of the non-invasively accessed body fluids and it may be the most common time-resolved (chronological) readings of biomarker concentrations compared to saliva and urine [13-15]. Biological tissues have a higher concentration of ions and water content than non-biological tissues. Because the interaction of microwaves with biological material at frequencies above about 100 MHz is almost totally dependent on the aqueous and ionic content, precise estimates of the complex permittivity of salt solutions at these frequencies are extremely significant. In lab tests to assess the dielectric properties of biological materials, NaCl in an aqueous solution is frequently used as a reference liquid [16]. Designing an antenna that can detect the change in electrolyte ion

concentrations by detecting the change in their dielectric properties will not only help in detecting electrolyte imbalance in a simple, non-painful way but also pave the way for a cheaper electrolyte detection method that is substantially cheaper and accessible than current alternatives. There are already many works done in the field of non-invasive electrolyte measurement such as micro-strip patch antenna [17], blood potassium concentration from ECG in hemodialysis patients [18], estimation of plasma sodium concentration during hemodialysis via capacitively coupled electrical impedance spectroscopy etc [19]. But most of the existing detection methods have some limitations such as their range of operation, unreliable results at particular operation ranges, errors etc. The purpose of this study is to consider micro-strip patch antennas of different sizes and shapes and compare their results for different parameters such as sensitivity, linearity and error for electrolyte measurement from sweat. The results of this study will help us to grasp how the change of different antenna parameters affects its sensing abilities. Changing concentrations of electrolyte ions cause changes in the dielectric parameters of those ions. This dielectric change causes a shift in the resonant frequency and reflection coefficient  $S_{11}$ . The change of resonant frequency and  $S_{11}$  can be used to detect changes in electrolyte concentrations [20]. In our study, we used both the resonant frequency and  $S_{11}$  to see how they change according to changing electrolyte concentrations in human sweat. We also observed how these parameter shifts are affected by the changing antenna parameters. A study conducted at PICU of SVPPGIP (SCB MC and Hospital), Cuttack showed that Patients with electrolyte abnormalities have a 27.9% mortality rate (around 3 times higher than patients with normal electrolyte level) [21]. This further emphasizes the morbid nature and effects of electrolyte imbalance. The proposed comparative analysis of different antenna sizes will help to detect electrolyte imbalance in early stages thereby reducing the mortality rate caused by it.

## **Objectives of this Research**

- I. To design a micro-strip patch antenna for electrolyte detection from sweat
- II. Analyze the same micro-strip patch antenna for various size and parameters and compare their sensitivity

- III. Analyze the same micro-strip patch antenna for various size and parameters and compare their linearity
- IV. Analyze the same micro-strip patch antenna for various size and parameters and compare their error.

### **1.3 Thesis Outline**

Subject to the research objectives and targeted contributions mentioned above, this thesis is outlined as follows:

Chapter 1 gives a brief introduction about the research work that was done including relevant definitions. It also explains the reasons behind this research and its significance. The goals of this research are also mentioned in this chapter.

Chapter 2 focuses on the literature review part of the research where various other works relating to micro-strip patch antenna, electrolyte measurement techniques, non-invasive measurement techniques, Sensor operation, sensor classification etc are mentioned. This part presents the related research upon which the foundation of this research is based on.

Chapter 3 is the methodology part. This part explains the steps, procedures and techniques used for the research. This part explains the antenna design that is taken as reference, how to change electrolyte concentrations, variation of antenna parameters, how sensitivity, linearity and error was calculated.

Chapter 4 is results and discussion part which focuses on the simulated and the analyzed results. This chapter has two major parts: Total size variation and feed line width variation. Each of these parts has three parts that are sensitivity, linearity and error analysis. It also focuses on the conclusions drawn from the results. This part summarizes and discusses the results.

Chapter 5 focuses on the future goals of this research work. Gives a brief summary of the research work and concludes it.

## **Chapter 2**

### **Literature Review**

## 2.1 Introduction to Micro-Strip Patch antenna

A micro-strip antenna is a form of antenna that is manufactured on a printed circuit board (PCB) by using photolithographic processes [22]. It serves as a built-in antenna. Microwave frequencies are where they're most commonly used. An individual patch antenna consists of a patch of metal foil in various shapes on the surface of a PCB and a metal foil ground plane on the opposite side. The bulk of micro-strip antennas are made up of a two-dimensional array comprising many patches. Foil micro-strip transmission lines are used to connect the antenna to the transmitter or receiver. A radiofrequency current is provided between the antenna and the ground plane.

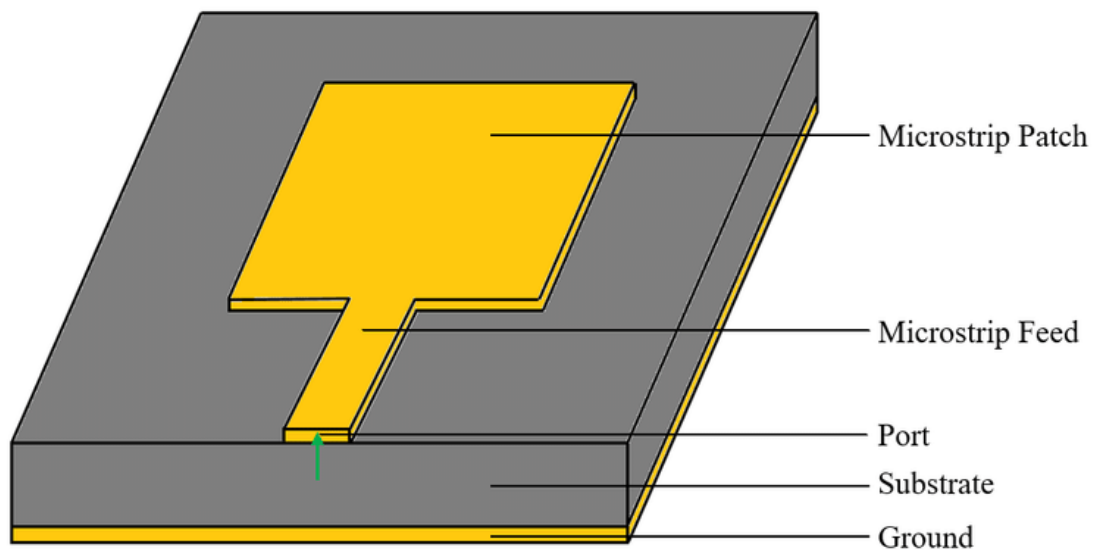


Fig. 2.1 Basic structure of a micro-strip patch antenna [23].

A micro-strip antenna's geometry consists of a dielectric substrate with a thickness  $d$ , complete metallization on one of its surfaces and a metal "patch" on the other. Typically, the substrate is thin. The metal patch on the front surface can come in a variety of shapes, but the most typical is a rectangular shape. Various ways can be used to excite the antenna. One popular method is to feed from a micro-strip line by attaching the micro-strip antenna to one of its edges at the center. The micro-strip line can be directly fed by connecting a signal source across the micro-strip line and the ground plane, or it can be connected to a feeding circuitry [24].

## 2.2 Use of Micro-Strip Patch Antenna in Biomedical applications

Micro-strip antennas are being more widely used in medical imaging, diagnosis, and treatment.

### **2.2.1 Breast Cancer Detection**

An improved E-shaped patch antenna was designed for better breast cancer detection. This work presents a flexible micro-strip antenna that can be placed in contact with the human body. Microwave breast imaging (MBI) uses small-power, extremely long radiation to gather information about breast tissues and its assurances to be a secure and more reliable modality for routine breast scanning. By locating the antenna in contact with the breast skin, the impact of signal interference from the breast skin is lowered. The surface of the antenna substrate could be considered a layer. Because of that, signal scattering from the skin is lowered and the transmitted signal is incinerated on the tumor, increasing tumor identification sensitivity [25].

### **2.2.2 Telemedicine and Electromagnetic Imaging Techniques**

Telemedicine and mobile healthcare communication systems necessitate compact antennas with better performance but smaller size and weight. A portable rectangular micro-strip antenna was established and used in a cancer detection study. The patch and ground portions of the antenna, which can be used as both a transmitter and a receiver in electromagnetic imaging techniques, are made of graphene, copper tape, conductive paint, and felt [26].

### **2.2.3 Medical Implant Communications Service**

A dual-band Micro-strip patch antenna for medical application has been developed, which can function in both the Medical Implant Communications Service with a frequency range of 402-405 MHz and the 2.4-2.5 GHz band selected from the Industrial Scientific and Medical bands (ISM). A rectangular radio wire with aspects of  $179.7 \times 228.3 \times 1.63$  mm was first reproduced to work in the MICS band and afterward another wandered serpentine shape, with a single feed point was utilized to extend the current path and cover both the MICS and ISM groups with new elements of  $31 \times 25 \times 1.63$  mm imprinted on 4.3 steady dielectric material [27].

### **2.2.4 Micro-Strip Patch Antenna for Health Care Monitoring**

The hexagonal micro-strip patch antenna is intended for use with a remote healthcare application. The coplanar waveguide (CPW) feed is used in the antenna because it can minimize back radiation and react at a wide bandwidth. The antenna usually measures 10 mm in length, 10 mm in width

and 1 mm in thickness. A hexagon shape antenna is designed and analyzed using skin, fat, muscle and also their relative dielectric properties, particle density and some specifications such as VSWR, return loss, gain and radiation pattern are measured. The measured return loss at a frequency of 2.25 GHz is 29 dB. Muscle, skin and fat have measurements of 0.8cm, 0.4 cm, and 0.4 cm respectively.

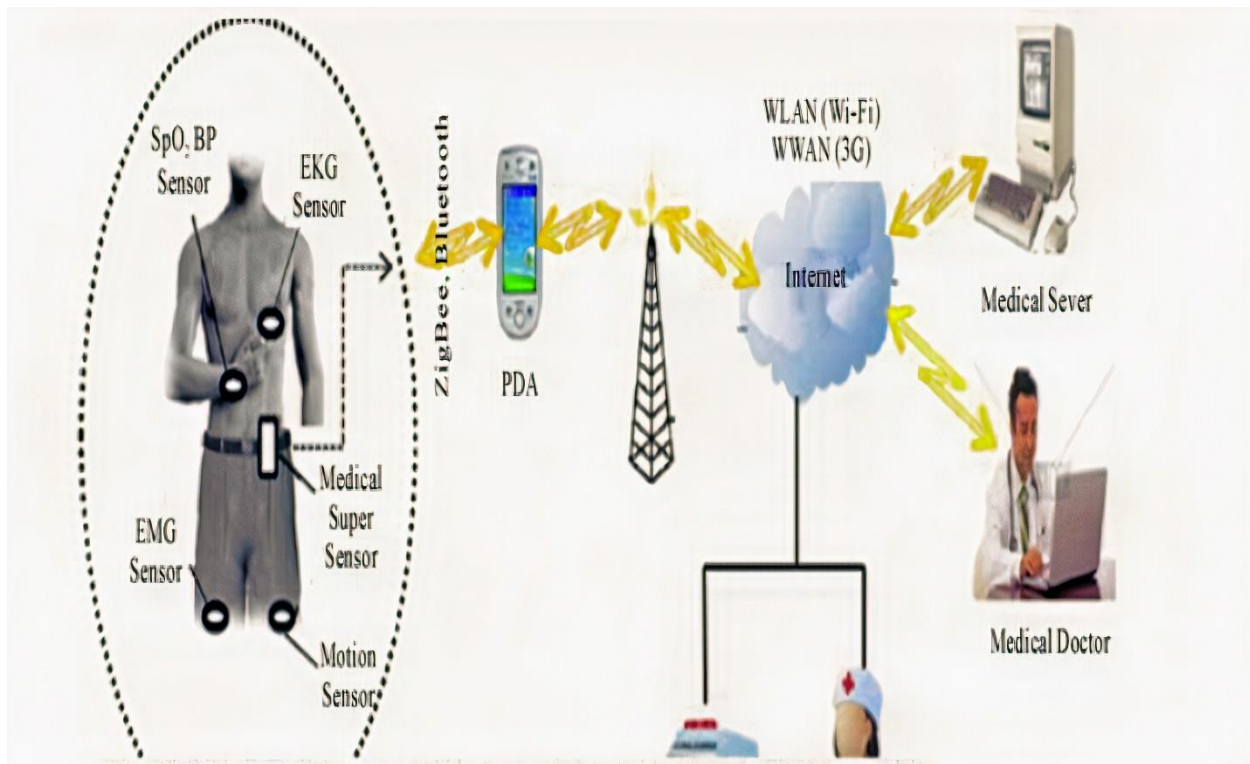


Fig 2.2: Wearable sensor for remote healthcare monitoring system

## 2.3 Various Electrolyte Measuring Techniques

### 2.3.1 Ion-Selective Electrode

In clinical medication, ion-selective potentiometry is as yet the strategy for decision for deciding electrolytes in different body liquids. This procedure has almost completely supplanted fire photometry and other recently proposed methods, for example, nuclear retention spectrophotometry and coulometry, for sodium, potassium and chloride particles ( $\text{Na}^+$ ,  $\text{K}^+$  and  $\text{Cl}$ ). An optimal ion-selective electrode (ISE) is comprised of a slim layer that permits simply the expected particle to go through. Although the electrodes measure a different amount the action, the outcomes for these electrodes are provided as concentrations. Direct ISE screens electrolyte action without weakening the sample and on second thought estimates electrolyte movement in plasma water ( $\text{mmol/kg H}_2\text{O}$ ) instead of plasma concentration ( $\text{mmol/L}$ ). A fixed multiplier, the activity coefficient, changes over the electrochemical action of the particles in the water to the readout concentration (Concentration = Activity coefficient). Nonetheless, focal labs as often as possible utilize backhanded ISE, in which the sample is weakened with a high-ionic-strength solution, bringing about an activity coefficient of one for every electrolyte. Aberrant tests useless plasma than direct measures, permitting multi-component analyzers to perform more examines per test and quicker robotized handling of various samples. In contrast, direct ISE responds to the electrolyte content of plasma water, whereas indirect ISE responds to the electrolyte content of the overall plasma volume [28].

### **2.3.2 Energy-Resolved Optical Non-invasive Electrolyte Detection**

Electrolyte balance should be checked consistently for people with Chronic Kidney Disease (CKD), particularly the individuals who are on dialysis. In the new COVID-19 pandemic, more extreme types of contamination have been accounted for in the old and those with co-morbidities like CKD. They are inclined toward COVID-19 as well as other medical clinic obtained diseases because of the intermittent blood tests for electrolyte balance observation (HAI). Therefore, a harmless methodology for identifying essential electrolyte ( $\text{K}^+$  and  $\text{Na}^+$ ) levels is critical. Analysts made a painless optical discharge spectroscopy-based framework for fast and dependable synchronous observing of salivary  $\text{Na}^+$  and  $\text{K}^+$  levels in a review. A shut flash chamber, miniature spectrometer, high-voltage flash generator, electronic circuits, optical fiber, and exclusively created programming in view of the LabVIEW stage contained the gadget. The optical emanation delivered from the organic example (i.e., salivation) attributable to recombination of particles animated by impingement of electrons getting back from a high voltage flash offers significant data in regards to the electrolyte concentration. A limited scale clinical exploration including 30 sound humans exhibits the gadget's true capacity for estimating salivary  $\text{Na}^+$  and  $\text{K}^+$  focuses. The minimal expense, convenient place of-care contraption just requires 2 mL of test and can test 0.001-0.19 M  $\text{Na}^+$  and 0.001-0.27 M  $\text{K}^+$  simultaneously [29].

### **2.3.3 NaLiK for Electrolyte Detection**

Electrolytes like sodium, potassium, magnesium, calcium, and different minerals are vital for keeping up with liquid equilibrium and homeostasis in the human body. They're likewise useful

biomarkers for translating the pathophysiology of an assortment of issues. Scientists have fostered a gadget using the fundamental rule of optical emanation spectroscopy (OES) for quick, dependable and synchronous evaluation of potassium (K<sup>+</sup>), sodium (Na<sup>+</sup>), lithium (Li<sup>+</sup>) and in human samples. For the concurrent recognition of explicit electrolytes, the nuclear emanation spectra of the particles are procured and examined during their change. The optical sign is gained and the electrolyte content is determined utilizing programming created in-house. In contrast with the typical ISE approach, the gadget shows a sensible relationship in straight relapse examination for the three electrolytes (changed R<sup>2</sup> upsides of 0.984, 0.954, 0.932, and for K<sup>+</sup>, Na<sup>+</sup>, Li<sup>+</sup>, and individually). The contraption utilizes a little measure of serum (100 L) and has a superb association with financially accessible costly gadgets for blood electrolyte examination, for example, a Blood Gas Analyzer and an Ion Selective Electrode. The minimal expense gadget was made in-house and can test every one of the significant electrolytes simultaneously [30].

### **2.3.4 Integrated Ion-selective Optode Sensor Cartridge for Direct Electrolyte Detection**

Analysts have made an incorporated optode sensor cartridge that identifies sodium, potassium, and chloride particles in blood plasma without the requirement for pH change. Each optode sensor is comprised of two layers: the optode and a dry cushion, which cooperate to present plasma that is liberated from platelets and sifted by a membrane filter. An impartial ion-selective optode is utilized in the optode layer, which is comprised of an ionophore, a pH pointer color (chromoionophore) and ionic added substances implanted in a plasticized polyvinyl chloride membrane. The dry support layer is added to the optode layer, which disintegrates when it comes into contact with plasma, bringing about a steady pH of the plasma inside the optode membrane. In light of the pK<sub>a</sub> of their related chromoionophores and powerful cushion ranges, we decided the pHs of each dry support (sodium, potassium, and chloride) layer to be 6.0, 7.0, and 4.5, separately. Thus, the sensor reactions differed relying upon the measures of potassium, sodium, and chloride particles [31].

### **2.3.5 Non-invasive Micro-strip patch Sensor for Electrolyte Detection**

Analysts have proposed a minimal expense non-invasive micro-strip patch antenna-based sensor to recognize electrolytes from human perspiration. A Copper patch radio wire with a frequency of 0.5 GHz to 3.5 GHz was developed as the sensor. The antenna is constructed from a 1.5 mm thick paper substrate. Whenever fluid is consumed by a substrate, its dielectric attributes are changed. For different concentrations of sodium chloride (NaCl) going from 0.05 mol/L to 0.3 mol/L, the magnitude of reflection coefficient and change in resonant frequency is noted. Since there is a significant change in both reverberation recurrence and size of reflection coefficients for shifted degrees of electrolytes, the primary reverberation is utilized for information examination. This copper patch antenna has been taken as the reference design for our micro-strip patch antenna analysis in this thesis project [17].

## **2.4 Non-Invasive Measurement Techniques**

### **2.4.1 Non-invasive Measurement of Blood Components**



The discoveries of in-vitro and in-vivo tests are furnished along with a sensor framework for estimating blood parts like hemoglobin. For these non-invasive optical measures, NIR-spectroscopy and Photoplethysmography (PPG) are used as the hidden innovation. The ingestion coefficient of blood in the noticeable and close infrared reaches is notable, and it is generally affected by the different hemoglobin derivatives. This data is utilized to register the optical absorbability properties of blood, which include information for blood parts such as arterial oxygen saturation (SpO<sub>2</sub>), hemoglobin (Hb), carboxy-hemoglobin (CoHb), and met-hemoglobin. A non-invasive innovation accommodates effortless persistent online patient checking with an okay of disease, as well as continuous information observing and clinical reaction to recorded information [32].

#### **2.4.2 Techniques for Non-Invasive Monitoring of Arterial Blood Pressure**

Checking blood vessel pulse (BP) is a backbone of hemodynamic observing in intensely or fundamentally sick patients. Hypotension and hypertension might conceivably think twice about the activity of significant organs like the heart, cerebrum or kidneys. Corridor pulse can be estimated obtrusively utilizing a blood vessel catheter or harmlessly with a finger stick. Discontinuous or ceaseless BP estimations are accessible with painless BP estimation. For discontinuous painless observing, a blocking upper arm sleeve is generally commonly used. The BP is then estimated either physically (utilizing Korotkoff sounds or palpation) or naturally (utilizing oscillometry, for example). The volume clip technique or blood vessel applanation tonometry can be utilized for ceaseless painless BP observing. The blood vessel waveform and circulatory strain estimations can be gotten continually utilizing the two systems [33].

#### **2.4.3 Non-Invasive Measurements in the Assessment of Bladder Outlet Obstruction**

The significance of genuine estimations in diagnosing the wellspring of lower urinary lot side effects (LUTS) is investigated. It goes over the customary strategies that are accessible, which are generally intrusive, before summing up the developing range of non-invasive estimation procedures. The highest quality level for arranging bladder outlet obstruction (BOO) is to utilize recorded bladder pressure and urinary stream rate during voiding in an obtrusive strain stream study. On the nomogram perceived by the International Continence Society, the conclusion is currently made by diagramming the detrusor tension at the greatest stream and most extreme

stream rate ( $Q_{max}$ ). The void will be delegated deterred, questionable, or unhampered in this format. On account of the obtrusive and complex nature of this review, various novel techniques have been created to order BOO, either by estimating bladder pressure harmlessly or by utilizing an intermediary measure, for example, bladder weight. Harmless methodologies for diagnosing BOO have shown critical potential and a couple has even arrived at the place of commercialization [34].

#### **2.4.4 Non-invasive spectroscopic techniques in the diagnosis of non-melanoma skin cancer**

Non-melanoma skin cancer is on the ascent all over the planet and they've turned into a significant issue to our wellbeing and financial concern. Skin malignant growth can be distinguished and treated early, which can further develop the patient's result decisively. Subsequently, the need for good administration and compelling non-invasive indicative strategies is expanding to limit backslides or superfluous treatments. Even though biopsy followed by histopathology assessment is as of yet the highest quality level for non-melanoma skin cancer diagnosis, optical non-invasive demonstrative techniques are acquiring prominence. Superior quality optical rationality tomography, fluorescence spectroscopy, and angled frequency diffuse reflectance spectrometry, among other spectroscopic strategies are arising non-invasive or negligibly intrusive methods with possible appropriateness in the determination of non-melanoma skin malignancies [35].

#### **2.4.5 Non-invasive measurements of carboxyhemoglobin and methemoglobin in children with sickle cell disease**

The estimation of oxyhemoglobin immersion in sickle cell disease (SCD) patients is critical for the early recognition of hypoxemia. Since carboxyhemoglobin (COHb) and methemoglobin (MetHb), decline the oxygen content of blood, the precision of heartbeat oximeter estimations of blood oxygenation in SCD patients is a shift. The exactness and unwavering quality of a non-invasive heartbeat co-oximeter in estimating COHb and MetHb rates (SpCO and SpMet) in kids with SCD were researched in a review. The assumption was that non-invasive heartbeat co-oximetry proportions of COHb and MetHb accord wiith adequate clinical precision with intrusive entire blood co-oximetry estimations. Fifty kids with SCD-SS had their heartbeat and blood oxygen levels estimated while space to breathe air. The aftereffects of non-invasive COHb and

MetHb measures were contrasted with blood estimations. For MetHb, the pulse co-oximeter bias was -0.22 percent, while for COHb, it was 0.1 percent. The deliberate SpCO had an accuracy of 2.1 percent inside a COHb scope of 0.4-6.1 percent, while the deliberate SpMet had an accuracy of 0.33 percent inside aMetHb scope of 0.1-1.1 percent. COHb and MetHb levels in kids with SCD were estimated utilizing non-invasive heartbeat co-oximetry. Notwithstanding the way that the harmless strategy to some degree misjudged obtrusive COHb measures and marginally underrated intrusive MetHb information, the two techniques were in close understanding [36].

## **2.5 Sensor Classification**

### **2.5.1 Electrochemical Sensors**

A detecting or working terminal, a reference electrode, and much of the time, a counter electrode makes up an electrochemical sensor. Normally, these terminals are in touch with either a fluid or a strong electrolyte. Electrochemical sensors are utilized to distinguish pH, conductivity, broke up particles and disintegrated gases at low temperatures (beneath 140° C). Strong electrolyte sensors are used for readings at high temperatures (>500° C), for example, exhaust gases and liquid metals [37]. Electrochemical sensors work by detecting an electrical boundary of the material is contemplated. They can be characterized by the strategy for estimation utilized.

Electrochemical sensors give a few advantages, including low power utilization, high responsiveness, high exactness, and protection from surface harming. Nonetheless, ecological factors, strikingly temperature, altogether affect their responsiveness, selectivity, and security. Natural variables impressively affect functional life expectancy; for instance, in hot and dry circumstances, a sensor's usable life will be enormously decreased. For gas sensors, cross-aversion to different gases can be an issue. The sensor's life expectancy can be abbreviated assuming that it is oversaturated with the types of interest. The most widely recognized electrochemical sensor types are displayed underneath:

### **2.5.2 Potentiometric Sensors**

This sensor identifies potential (voltage) changes between the functioning electrode and a reference electrode. The capability of the functioning is still up in the air by the concentration (or,

all the more exactly, the particle action) of the types of interest [38]. The electric potential framed between the functioning electrode and the reference electrode in a pH sensor, for instance, is a component of the pH worth of the liquid being estimated. Particle-specific cathodes for both inorganic (for instance, checking metal particle contamination in natural examples or profiling of blood electrolytes) and natural particles (for instance, fragrant aldehyde or ibuprofen in human serum tests) are further purposes of potentiometric sensors.

### **2.5.3 Amperometric Sensors**

This sort of electrochemical sensor recognizes current vacillations. The functioning terminal's true capacity is held steady (in contrast with a reference anode), and the current is checked over the long run. Redox (decrease oxidation) processes at the terminal surface are driven by the applied voltage and direct electron transport (current) [39]. The functioning terminal is set up so the deliberate current is corresponding to the centralization of the redox dynamic species in the example arrangement. Oxygen detecting (PO<sub>2</sub> and PCO<sub>2</sub> patient observing), fire discovery (for instance, CO from seething flames) and harmful gas location (for instance, chlorine (Cl)) are normal purposes.

### **2.5.4 Coulometric**

Coulometric sensors measure how much power is delivered by an electrochemical response in coulombs. This is achieved by keeping a steady voltage on a functioning electrode and checking the current moving through a related circuit. At the electrode, the analyte of interest is oxidized or diminished. The current being observed downfalls as the analyte is consumed, in the end reaching at zero. e speed at which the analyte is shipped to the functioning terminal decides the response rate. A rendition of this arrangement is used in some oxygen sensors, where both a cathode and an anode are utilized with a DC voltage kept up between them. Through a permeable layer, oxygen particles from the sample diffuse to the cathode, where they are reduced. O<sub>2</sub>-particles are drawn to a strong electrolyte that has been warmed to 400°C. At the anode terminal, the oxygen particles are changed back to sub-atomic oxygen.

Coulometric sensors can likewise be utilized to identify glucose. Since the compound used in the sensor, glucose oxidase, is specific for glucose, the entire charge recorded by the sensor compares

to the all-out concentration of glucose in the sample — as long as the enzymatic response is finished. The way that no adjustment is important for this underutilized approach is gigantic in addition; you should simply count the electrons and make an interpretation of it how many glucose particles. The gadget for on-body detecting or embedded sensors is extensively improved by taking out the prerequisite for alignment [40].

Coulometric sensors enjoy a few upper hands over amperometric sensors, including expanded responsiveness, selectivity, and solidness. One more significant advantage of this sensor is that it might give outright quantitation whenever used fittingly. The relating charge is an outright proportion of sum and fixation assuming the sensor's cell volume is known and the types of interest is completely electrolyzed [41].

### **2.5.5 Conductometric Sensors**

This sort of sensor chips away at the hypothesis that electrical conductivity can adjust in the presence or nonattendance of specific synthetic species. There are two routinely utilized setups. A delicate directing layer and contact electrodes make up the main design. The resistance of the sensor is estimated after a DC voltage is applied. Chemiresistors in gas-detecting applications frequently has this plan. The directing layer can be either a permeable thick film (0.002-0.3 m) that permits the gas to diffuse through it, bringing about high responsiveness or a meager film on which the source material is faltered (a cycle wherein molecules are shot out from an objective or source material and saved onto a substrate) or kept utilizing compound fume statement onto a substrate layer, bringing about high awareness [42]. In the subsequent plan, the analyte of interest is acquainted with an electrolytic arrangement that contains a electrode (regularly glass) with an artificially collaborating layer on top. To finish the circuit, a counter electrode is used. Biosensors much of the time utilize this arrangement. Conductometric sensors are famous in light of the fact that they are frequently reasonable.

## **2.6 Sensor Characteristics**

## 2.6.1 Sensor Sensitivity

The adjustment of information expected to deliver a unit change in yield is known as sensitivity. Assuming the sensor reaction is direct, the sensitivity will be consistent across the sensor's reach and equivalent to the straight-line plot's slope. An ideal sensor will have high and steady sensitivity. Say  $S$  is a polynomial equation whose value is

$$S = P.x^3 + Q.x^2 + R.x + C \quad (2.1)$$

Where,  $P$ ,  $Q$ ,  $R$ ,  $C$  is constant. The derivative of  $S$  with respect to  $x$  ( $dS/dx$ ) can be calculated if the sensor response is non-linear. Dead-bands and immersion are two normal sensitivity-related concerns. The dead-band is a scope of info signals where the sensor is harsh or lethargic. Over the entire dead-band zone, the result might stay almost a given worth (normally zero) there. By and large, dead band is expressed as a level of length. The info esteem at which no further changes in result might happen is known as the immersion point [43].

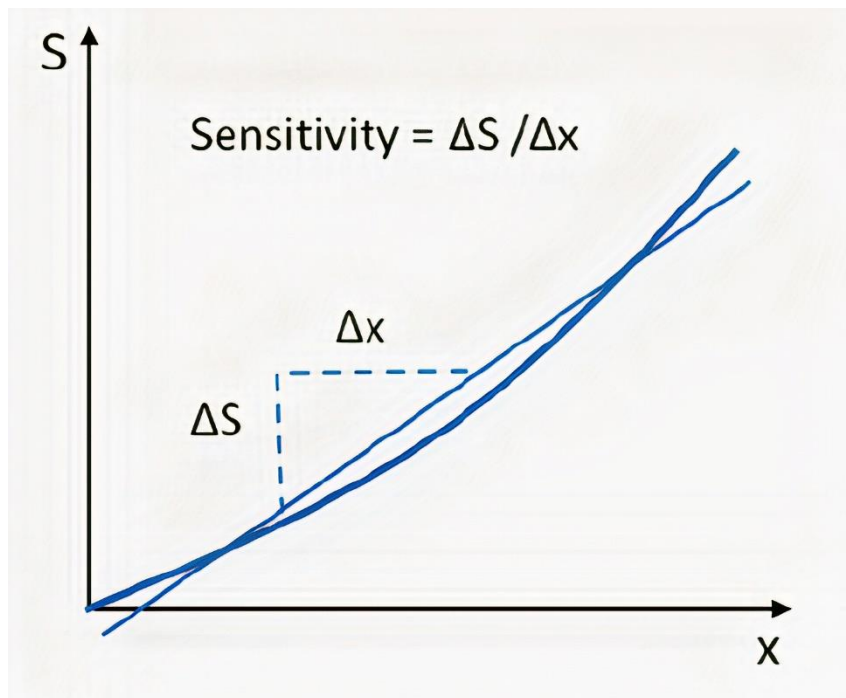


Fig 2.3: Sensor sensitivity [43].

## 2.6.2 Sensor Linearity

Sensing devices are vital for different framework computerization and observing of different physical and substance boundaries. Nonlinearity has been a well-established worry for most sensors, consequently, numerous linearization techniques have been introduced in a review to address it. The sort and nonlinearity worth of the sensor output decide the exactness of linearization frameworks. Since it is challenging to get a precise polynomial condition or another capacity to portray the reaction bend, the estimation boundary is inferred utilizing backward guess capacities, which brings about additional inaccuracy. The linearized properties will facilitate the plan, alignment and estimation exactness on the grounds that numerous sensors are utilized for different applications. Simple methodologies are as yet famous among numerous scholastics because of the accessibility of superior execution simple equipment. Be that as it may, as IC advancements progress, equipment execution of programming techniques might be done rapidly, efficiently and with more accuracy, permitting computerized strategies matched with programming ways to deal with achieve the work with more noteworthy adaptability and productivity [44].

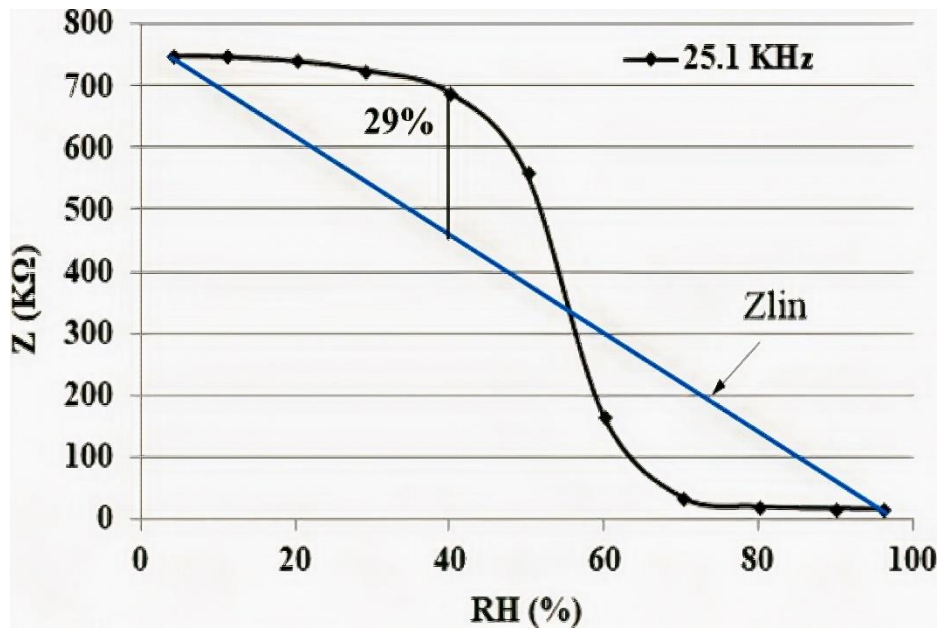


Fig 2.4: Sensor Linearity [44].

### 2.6.3 Error

The inconsistency between the deliberate value and the genuine value, where real value alludes to a flat-out or settled upon standard, is called error. An error might be grouped into two kinds: precise and arbitrary [22].

### **Systematic Error**

Systematic errors are repeatable mistakes that can be compensated for through techniques like feedback, filtering, and calibration [45].

### **Random Error**

A signal component that conveys no data is known as random error (otherwise called noise). The signal-to-noise ratio (SNR), which is the proportion of the authentic sign abundancy to the clamor standard deviation, is a quantitative proportion of signal quality. A high signal-to-noise ratio (SNR) indicates great signal quality. Noise can be evaluated by keep the signal without the measure and or by over and again recording a known measure and deducting the known genuine signal from the deliberate signal. The relative standard deviation of the sign sufficiency used to measure accuracy is contrarily corresponding to SNR. As an outcome, a noisy signal is additionally a signal that is uncertain.

## **Chapter 3**



# Methodology

## 3.1 Introduction

In this study, we did a comparative analysis for a reference antenna for two different kinds of dimension variation. One is total size variation and the other is feed-line width variation. In the case of total size variation, all the parameters were varied but in the case of feed-line width variation, only the width of the feed-line was varied. While experimenting with both of these cases we utilized 5 different antenna sizes which were a 20% increase, 10% increase, actual size, 10% decrease and 20% decrease for total size variation. For feed-line width variation, we kept all the antenna parameters the same but only varied the feed-line width. We used five different sizes of feed-line width which were 20% increase, 10% increase, actual size, 10% increase and 20% increase. We used eight different concentrations of NaCl solution for this study which were 0.01, 0.03, 0.05, 0.07, 0.09, 0.1, 0.15, 0.2 mol/L.

All of the different antenna sizes and parameters were simulated for eight different concentrations of NaCl solutions in COMSOL Multiphysics software. We used frequency sweeping for our simulation. We used a frequency range of 0.1GHz-2GHz. After simulating all the antennas of different sizes and parameters we calculated their various characteristics such as sensitivity, linearity and error.

The entire research was done in two parts. First, the frequency sweep was done for all five sizes for total size variation from 0.1GHz-2GHz. Then three different characteristics such as sensitivity, linearity and error were calculated. For the linearity part for total size variation, the curves were divided into two parts. One ranging from 0.01GHz-0.09GHz and the other ranging from 0.09GHz-0.2GHz. This was done to increase the accuracy of the linearity equations. The same process was followed for the feed-line width case. For the error part, we chose 0.062 mol/L as the reference because it is the average NaCl level in sweat in an adult human. A flow chart summarizing the entire methodology is given below:

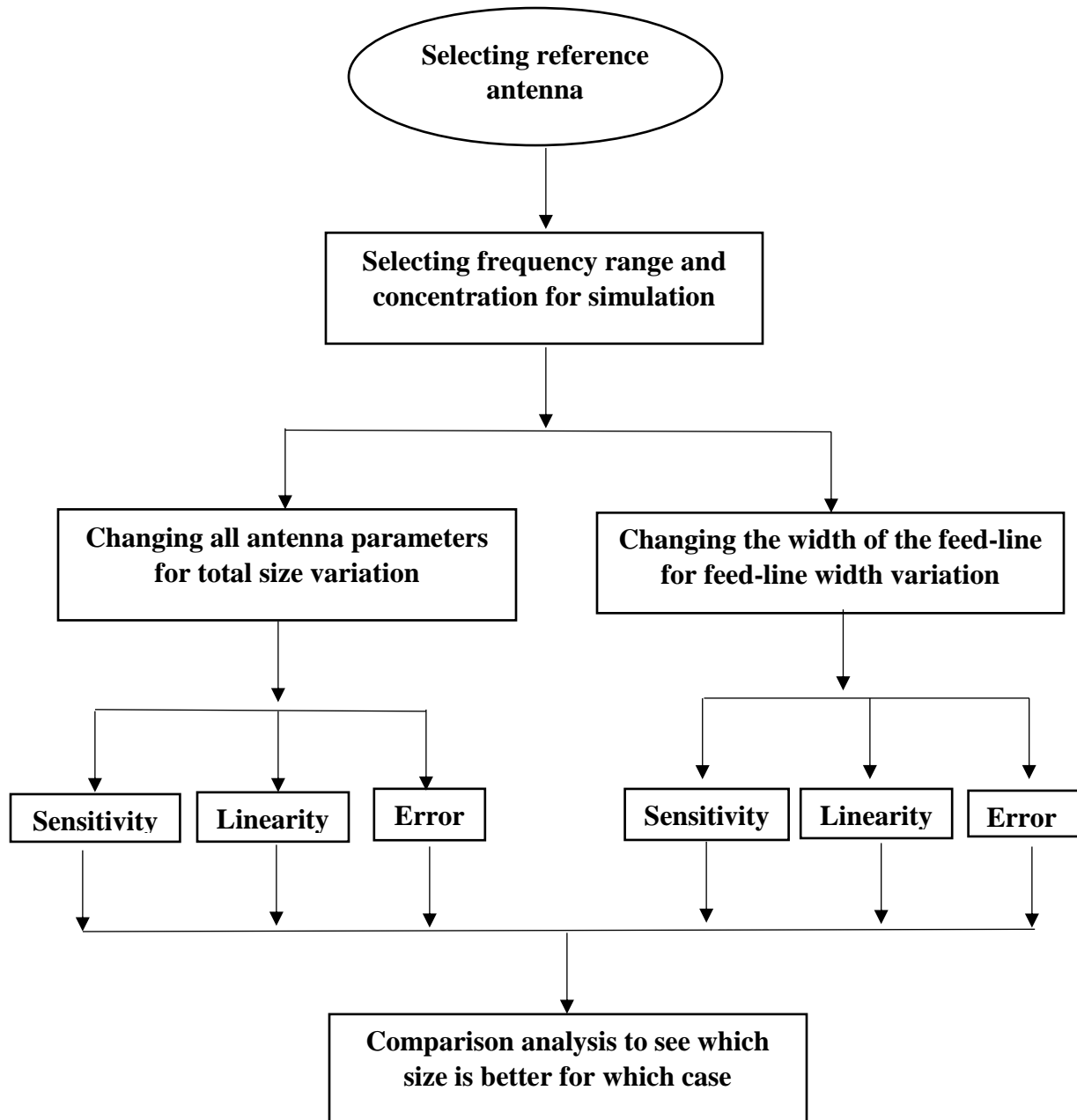


Fig 3.1: Flowchart

### 3.2 Reference design

For this study, a low-cost antenna-based sensor has been used as a base which is a 95 mm × 93 mm copper patch antenna with the paper substrate [46]. This is a three-layer antenna design that was simulated in the electromagnetic wave and frequency domain in COMSOL Multiphysics software. The three layers used for the design are a copper-based patch, a solid aluminum oxide (Al<sub>2</sub>O<sub>3</sub>) paper substrate, and a ground plane. The entire patch and substrate were covered with liquid NaCl as a substitute for electrolyte solution from sweat. The design showed a resonant frequency vs reflection coefficient (S<sub>11</sub>) curve that serves as the basis of our study. The purpose of this study is to observe the change of concentration of NaCl by change of various electromagnetic values of the antenna. The higher rate of change means better detection capability of the antenna. To do this antennas of various sizes are compared to see which gives the best result. A reference patch antenna is taken as a base for this comparison.

### 3.3 Electrolyte solution concentration

For the next part of our analysis, we tested the base antenna design for eight different NaCl concentrations by using permittivity and conductivity values from [47].

**Table 3.1:** Dielectric Parameters of NaCl Concentrations at 20°C

NaCl (mol/L)	Relative Permittivity ( $\epsilon_r$ )	Conductivity ( $\sigma_i$ ) S/m
0.01	80.1	0.11
0.03	80.2	0.30
0.05	80.1	0.49
0.07	78.9	0.72
0.09	78.4	0.94
0.1	78.2	0.96
0.15	76.45	1.44
0.2	77.0	1.83

The change of dielectric values results in a change in the electromagnetic properties of a sensor which is observed in sensors' reflection-based parameters such as S<sub>11</sub> [48]. These changes in reflection-based parameters are used to detect the change in NaCl concentration in sweat.

### 3.4 Change of antenna parameters

In the next step, various antenna parameters were varied to see which variant gives better results in terms of sensitivity, linearity, and error. First, the antenna dimensions were varied based on their total size or in other-words all the parameters were varied. All the parameters were increased 10%, increased 20%, decreased 10%, and decreased 20%. These variations in parameters were done for all eight concentrations.

**Table 3.2:** Changed antenna parameters (in mm)

Parameters	Original value	10% increase	20% increase	10% decrease	20% decrease	Description
h	1.5	1.65	1.8	1.35	1.2	Thickness of substrate
W <sub>S</sub>	130	143	156	117	104	Width of substrate
L <sub>S</sub>	130	143	156	117	104	Length of substrate
W <sub>P</sub>	95	104.5	114	85.5	76	Width of patch
L <sub>P</sub>	93	102.3	111.6	83.7	74.4	Length of patch
W <sub>SB</sub>	7	7.7	8.4	6.3	5.6	Stub width
L <sub>SB</sub>	16	17.6	19.2	14.4	12.8	Stub length
W <sub>L</sub>	3.2	3.52	3.84	2.88	2.56	Feed-line width

Now in the same way we vary the feed-line width while keeping every other parameter the same as the base model. Here instead of changing all the parameters, we are only changing one parameter.

**Table 3.3:** Changed antenna feed-line width parameters (in mm)

Parameters	Original value	10% increase	20% increase	10% decrease	20% decrease	Description
W <sub>L</sub>	3.2	3.52	3.84	2.88	2.56	Feed-line width

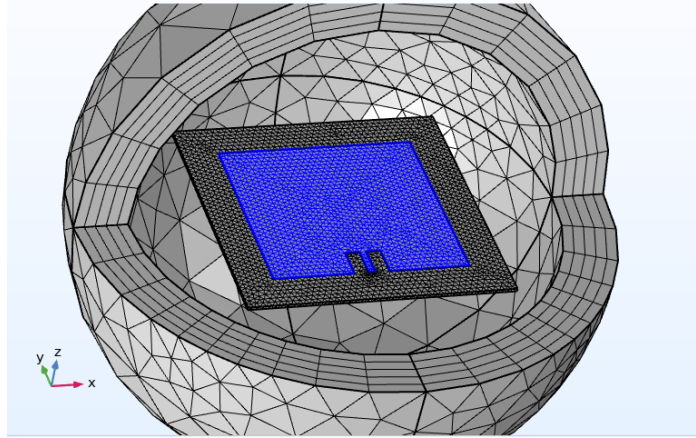


Fig. 3.2: Micro-strip Patch antenna design

### 3.5 Sensitivity comparison

Microwave frequency sensors are used for their ease of fabrication, small footprint, and real-time sensing capabilities [49-55]. Microwave sensors use high electric field concentrations to detect various changes in material properties and thus detect the material itself in real time [56]. This principle is used to detect the change in NaCl concentration from the change in resonant frequency and reflection coefficient ( $S_{11}$ ) [57]. NaCl concentration is taken x-axis and resonant frequency in the range of 0.01 GHz-2.0 GHz is taken as y-axis. The slope of this curve is considered to be the sensitivity of the antenna. The same is done for the reflection coefficient case where instead of resonant frequency  $S_{11}$  in dB is taken as the y-axis and everything remains the same. Then two methods of calculating sensitivity are compared to see which gives higher values.

### 3.6 Linearity comparison

In addition, to sensitivity one other parameter that plays a vital role in an antenna's sensing capabilities is its linearity. The sensitivity curves acquired from resonant frequency vs. NaCl concentration and reflection coefficient ( $S_{11}$ ) vs NaCl concentrations are converted into higher-order algebraic equations to express the antenna's electromagnetic shift characteristics in a mathematical form. The concentration of NaCl is made an independent variable and resonant frequency and reflection coefficient are kept as a dependent variable. The curves that are too nonlinear are divided into multiple equations for different frequency ranges to give a better

approximation. This way antennas of different parameters are compared to see which gives better results in terms of linearity.

### **3.7 Error comparison**

Finally, antennas of different parameters are compared for their errors. A random concentration of about 0.62mol/L is selected and put into the higher-order algebraic equations obtained from linearity analysis to calculate resonant frequency or reflection coefficient ( $S_{11}$ ). The same concentration is used in COMSOL to calculate the same parameters to see how much the simulated results vary from the results obtained from the equations.

## **Chapter 4**

## Results and Discussion

### 4.1 Total size variation of MPA-based sensor

Changes in the design of the MPA-based sensor can vary the results in a different manner. By decreasing & increasing the size of the proposed antenna, changes can be obtained which are shown in the following part.

#### 4.1.1 Sensitivity

Figures 4.1 and 4.2 delineate the resonant frequency and reflection coefficient ( $S_{11}$ ) of the sensor regarding NaCl concentration in sweat separately. It was examined that there was a huge change in the reflection coefficient and resonant frequency of the sensor because of the variety in NaCl concentration for various sensor sizes. The direct relapse examination was applied to the deliberate information and a decent relationship was seen between the s-parameter and NaCl concentrations.

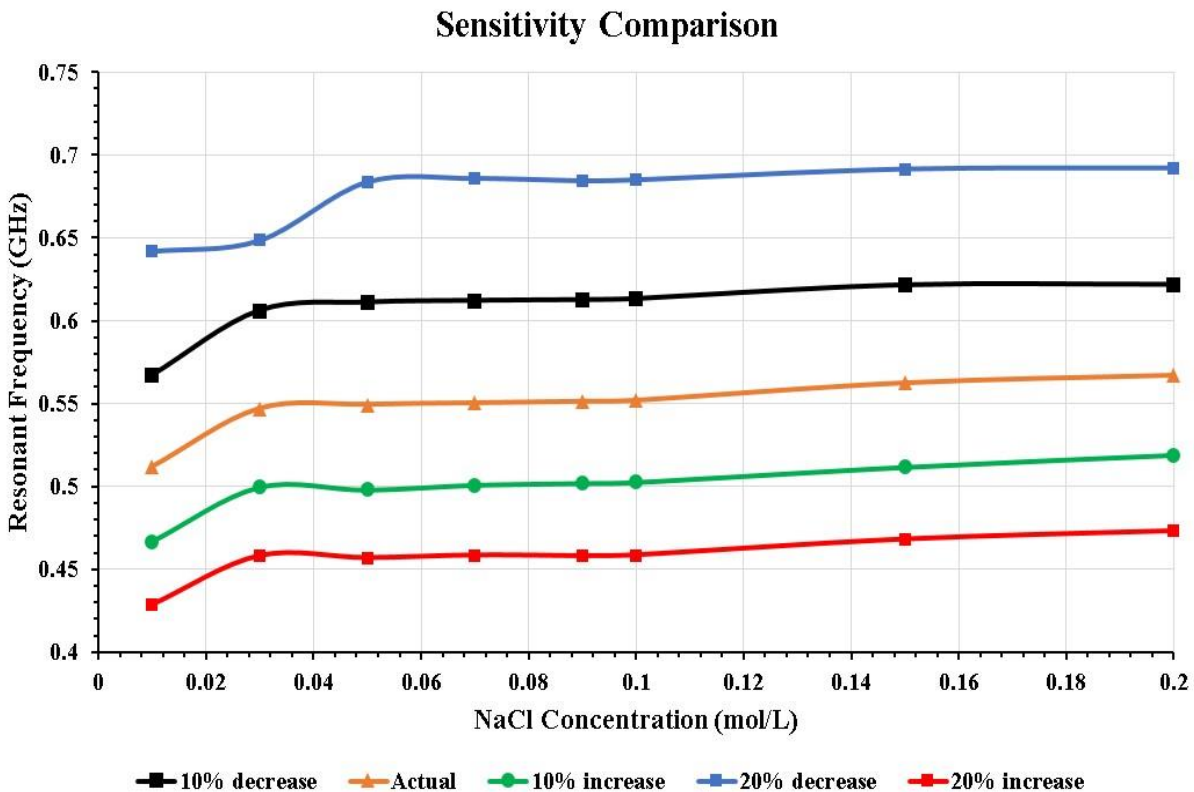


**Fig 4.1:** Resonant frequency vs NaCl concentration curve for five different MPA-based sensor size.

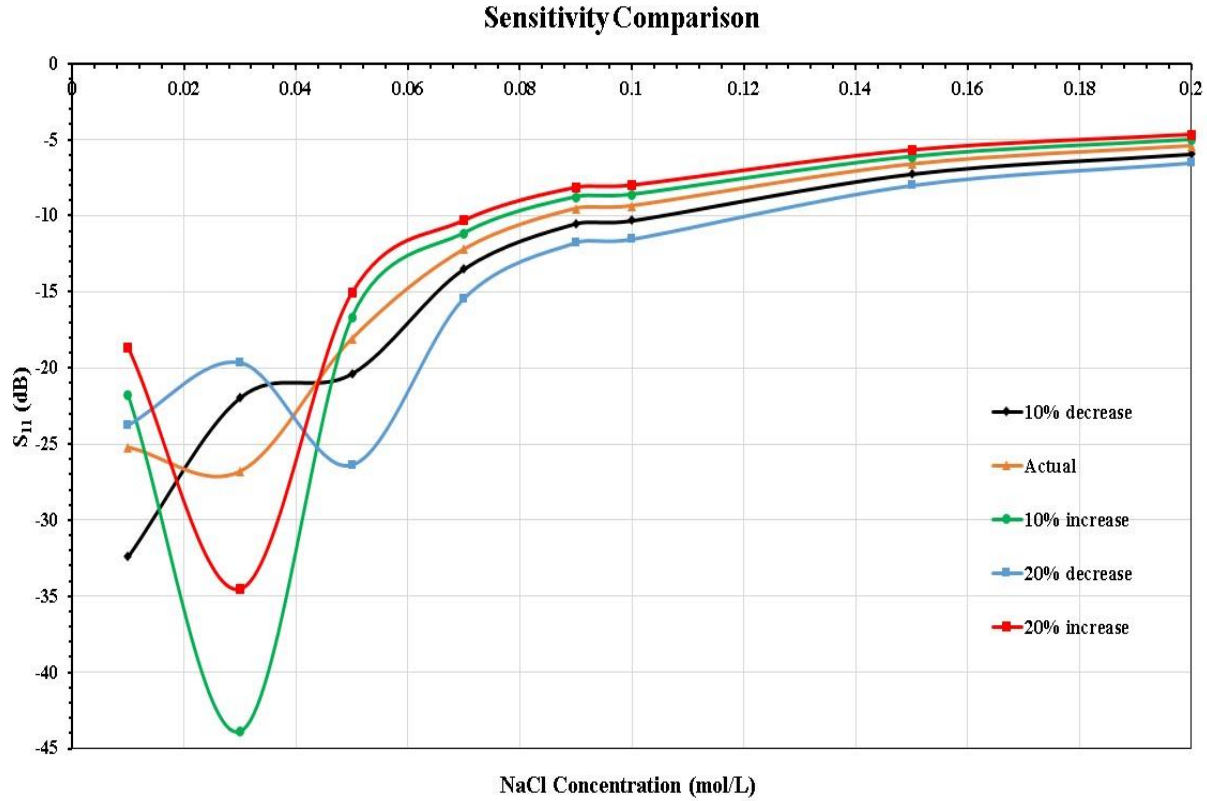


**Fig 4.2:** Reflection co-efficient ( $S_{11}$ ) vs NaCl concentration curve for five different MPA-based sensor size.

For total size variation, a sensitivity table is presented below. It can be observed that due to the variation in antenna sizes the slopes of the sensors are changed. From these slopes we can ascertain how changing the size of the sensors affects their sensitivity.

**Table 4.1:** Sensitivity Table (Total size variation)

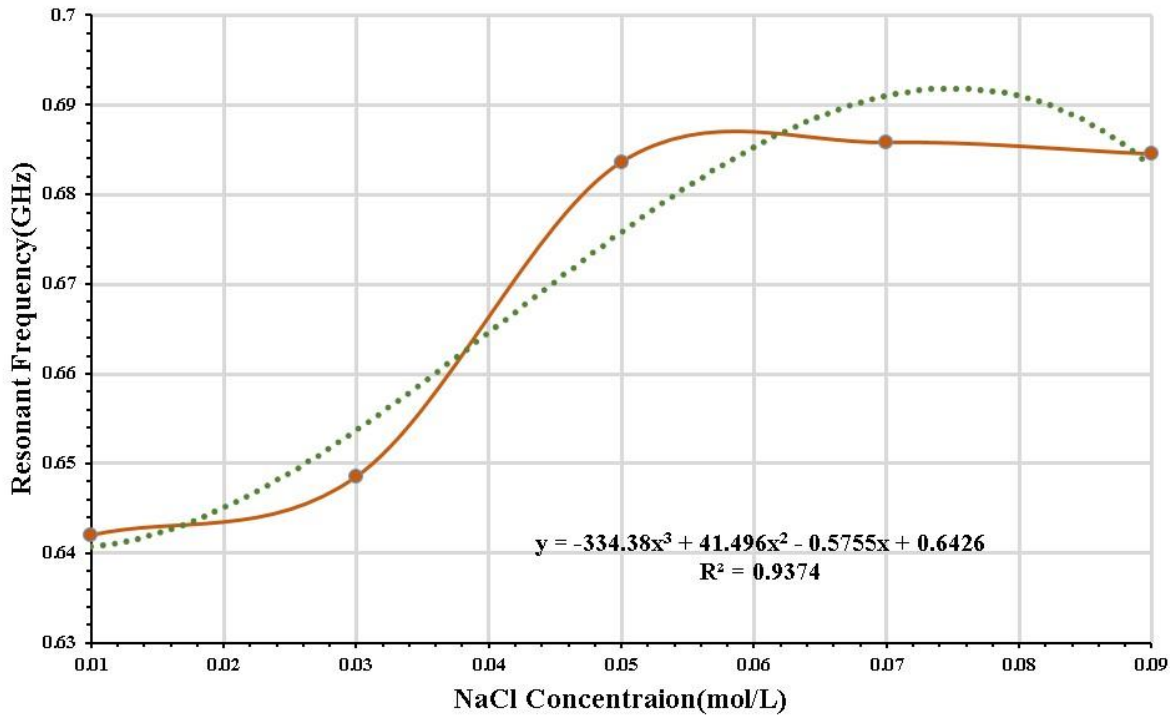
SI No.	Parameters	Concentration (mol/L)	Frequency (GHz)	$S_{11}$ Parameter (dB)	Sensitivity Slope (in terms of freq shift)	Sensitivity Slope (in terms of $S_{11}$ shift)
1.	20% decrease	0.01	0.6420	-23.772	0.2409	99.658
		0.03	0.6485	-19.656		
		0.05	0.6836	-26.395		
		0.07	0.6858	-15.450		
		0.09	0.6845	-11.7702		
		0.1	0.6850	-11.5467		
		0.15	0.6915	-8.014		
		0.2	0.6922	-6.528		
2.		0.01	0.5672	-32.39		



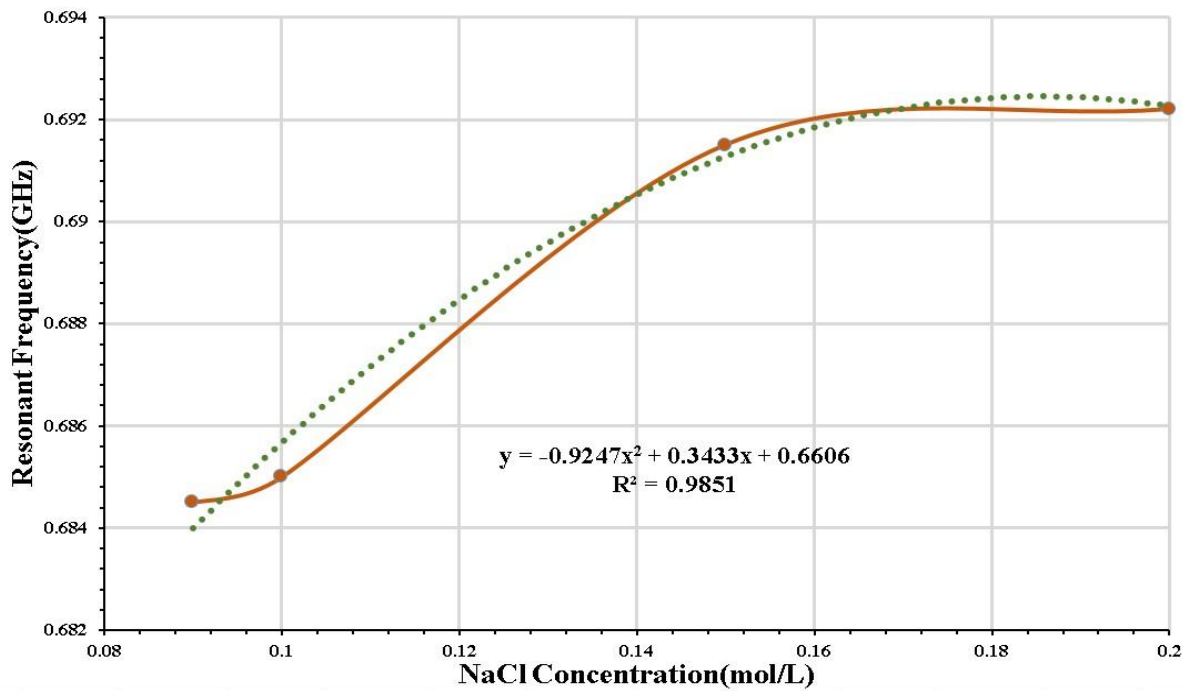
	10% decrease	0.03	0.606	-21.947	0.1979	94.778
		0.05	0.611	-20.365		
		0.07	0.612	-13.49		
		0.09	0.6125	-10.506		
		0.1	0.6131	-10.31		
		0.15	0.6213	-7.25		
		0.2	0.6216	-5.94		
3.	Actual Size	0.01	0.5116	-25.214	0.2111	107.325
		0.03	0.5468	-26.796		
		0.05	0.5493	-18.082		
		0.07	0.5502	-12.214		
		0.09	0.5511	-9.535		
		0.1	0.5517	-9.36		
		0.15	0.5622	-6.631		
4.	10% increase	0.01	0.4668	-21.826	0.2004	161.696
		0.03	0.4996	-43.9		
		0.05	0.498	-16.69		
		0.07	0.5009	-11.157		
		0.09	0.502	-8.784		
		0.1	0.5026	-8.628		
		0.15	0.5117	-6.14		
5.	20% increase	0.01	0.4284	-18.66	0.1707	128.414
		0.03	0.458	-34.50		
		0.05	0.4568	-15.06		
		0.07	0.4584	-10.312		
		0.09	0.458	-8.15		
		0.1	0.4585	-8.002		
		0.15	0.468	-5.7		
		0.2	0.473	-4.68		

#### 4.1.2 Linearity

For the linearity property calculation for different antenna sizes, we've used two kinds of graphs which are Resonant frequency vs. NaCl Concentration and  $S_{11}$  vs. NaCl Concentration. After that, the error is calculated between the results obtained from the software and the results obtained from the equations.

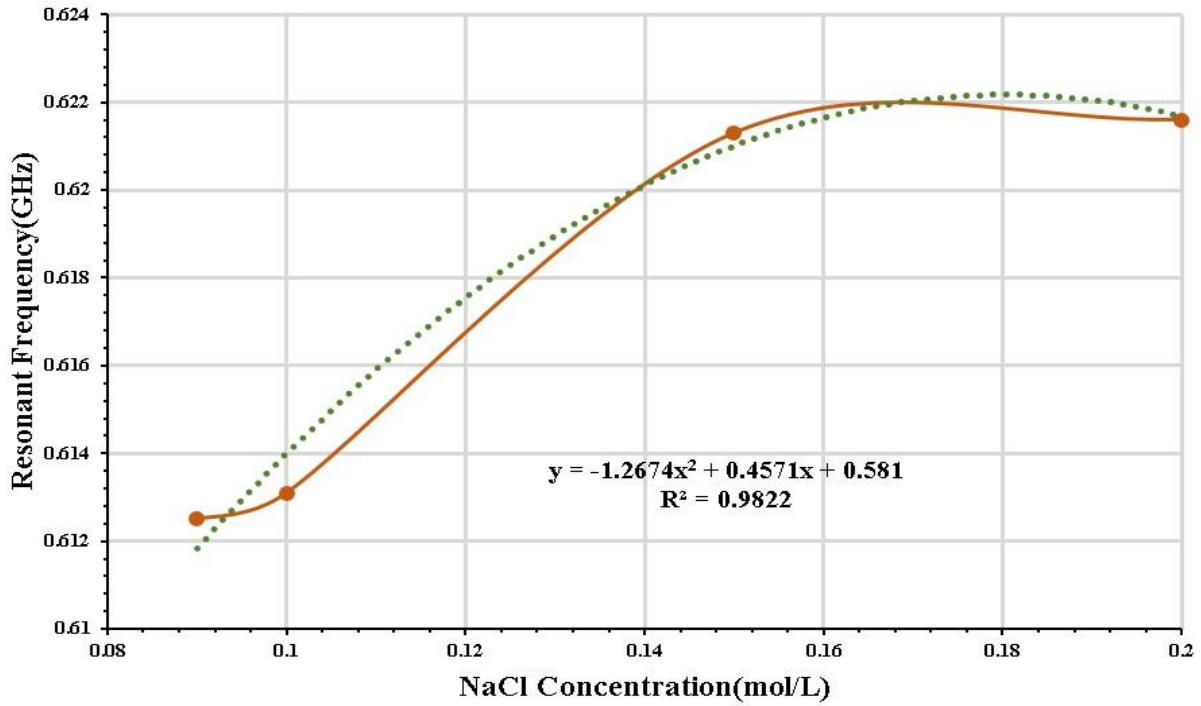


(a)

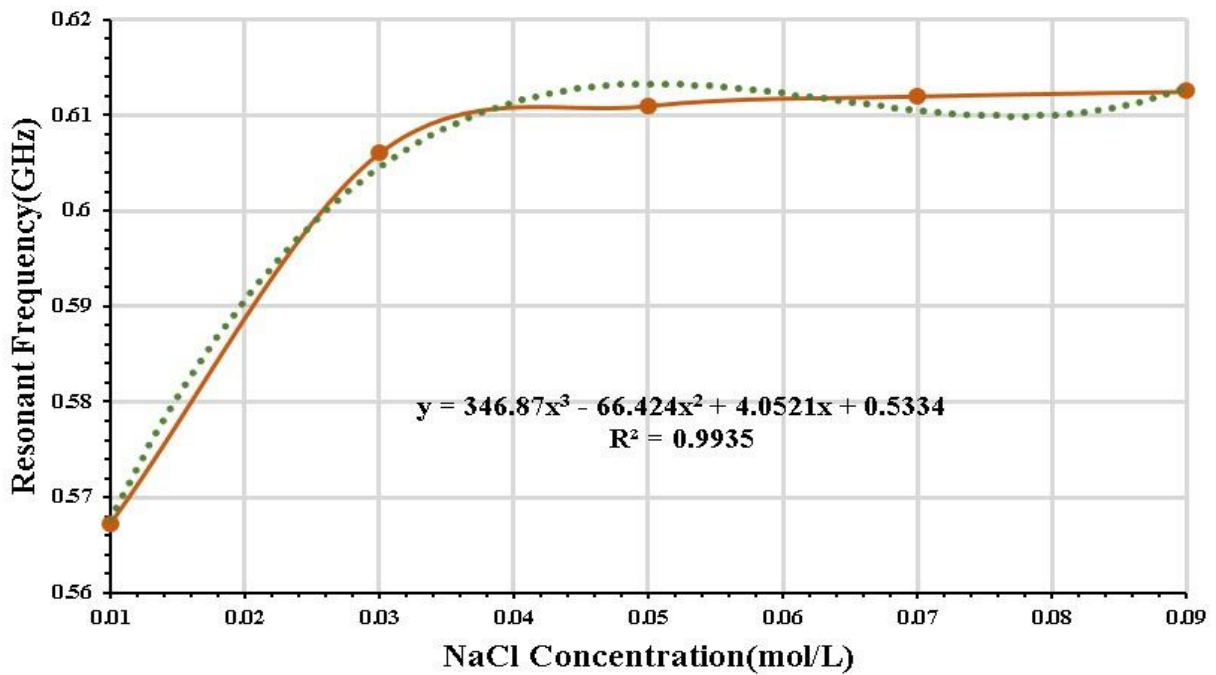


(b)

**Fig 4.3:** Frequency Vs Concentration for 20% decrease antenna size (a) from 0.01 to 0.09 mol/L NaCl concentration (b) from 0.09 to 0.2 mol/L NaCl concentration.

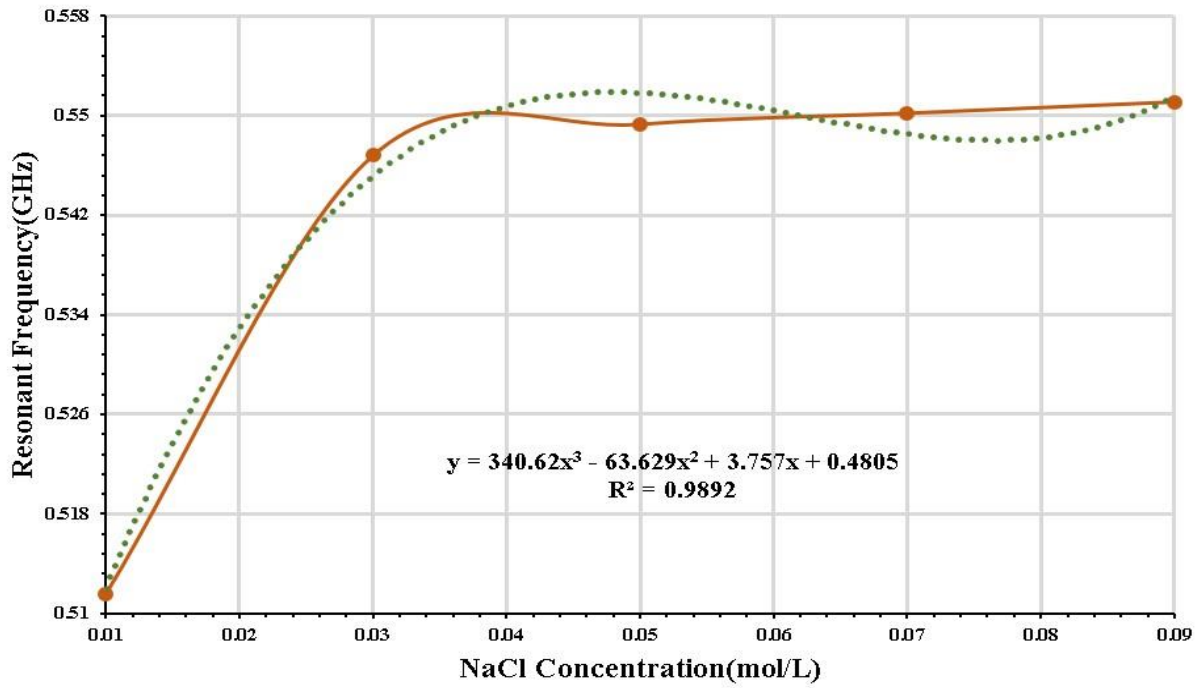


(a)

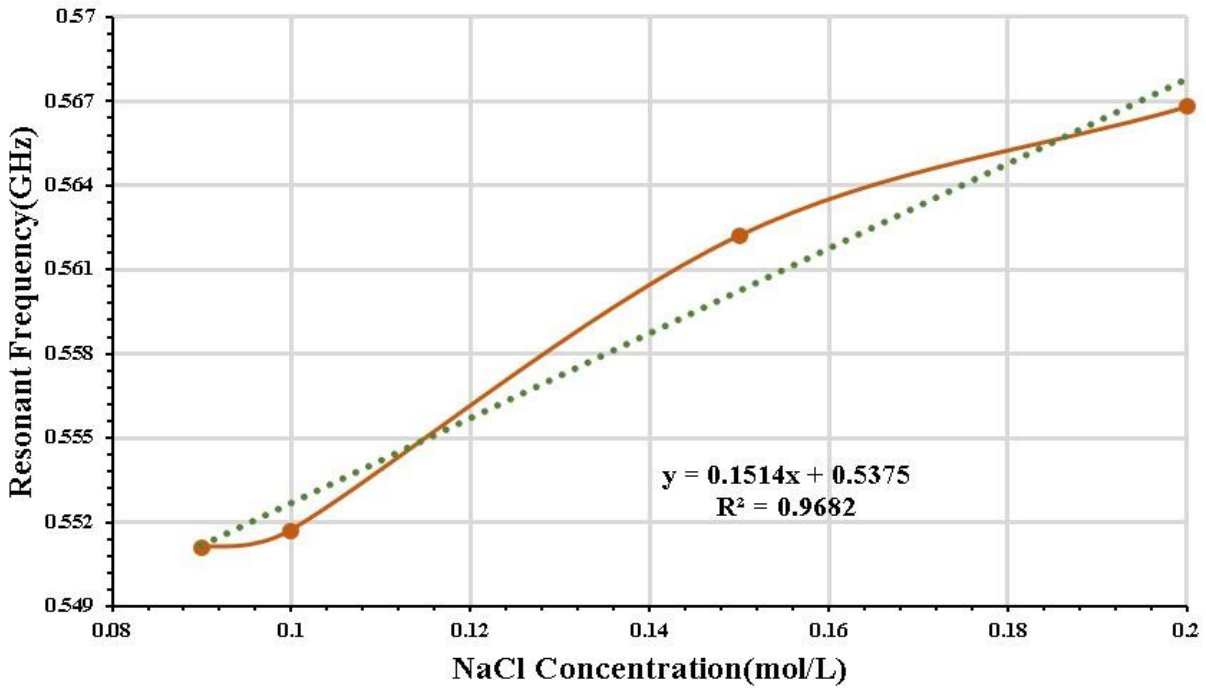


(b)

**Fig 4.4:** Frequency Vs Concentration for 10% decrease antenna size (a) from 0.01 to 0.09 mol/L NaCl concentration (b) from 0.09 to 0.2 mol/L NaCl concentration.

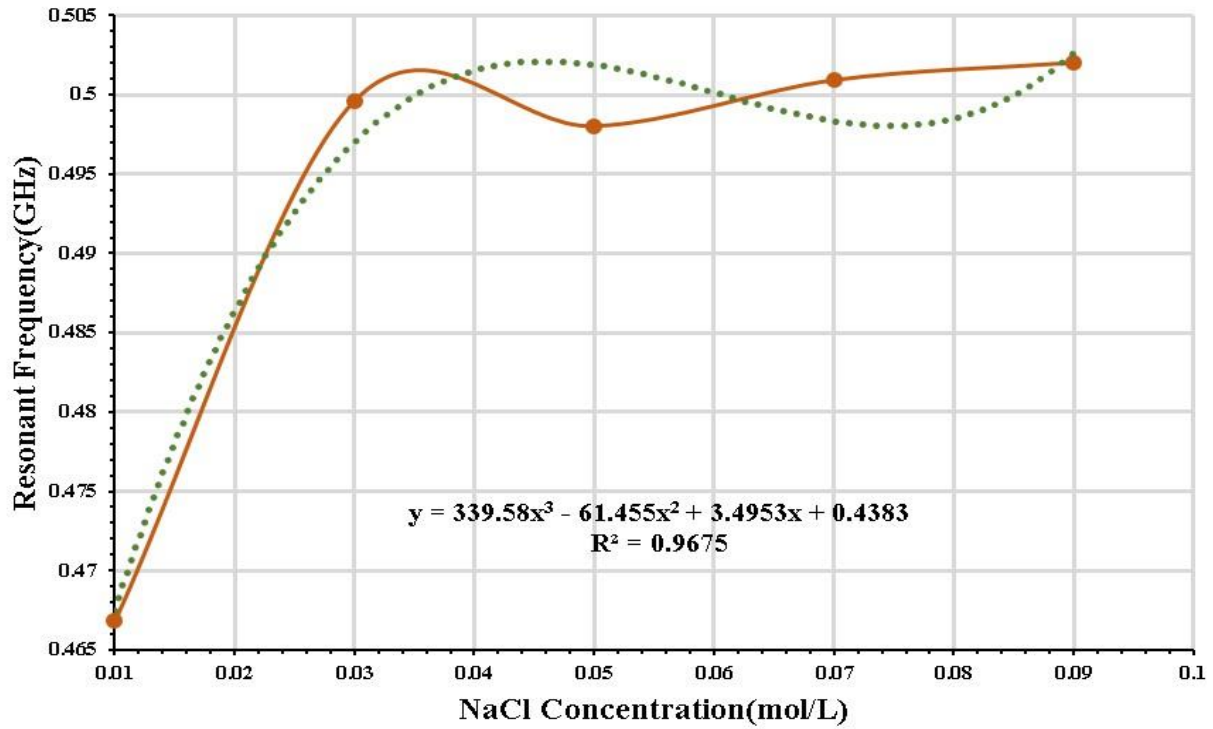


(a)

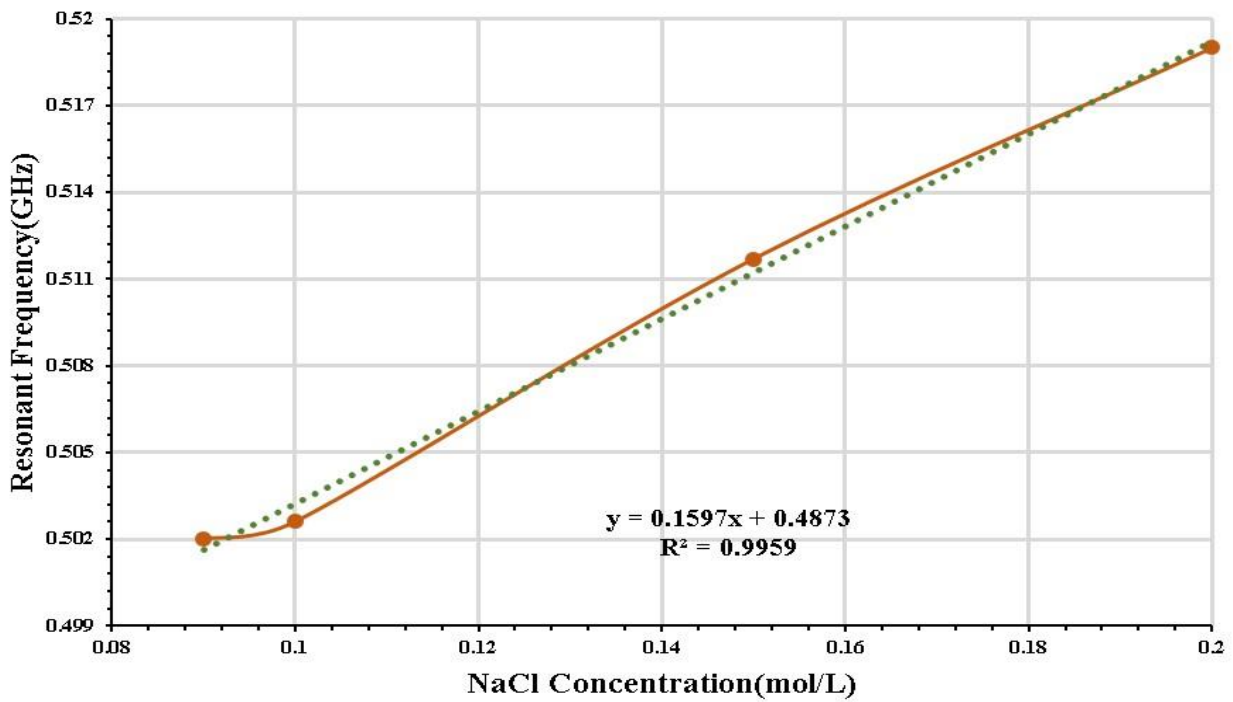


(b)

**Fig 4.5:** Frequency Vs Concentration for actual antenna size (a) from 0.01 to 0.09 mol/L NaCl concentration (b) from 0.09 to 0.2 mol/L NaCl concentration.

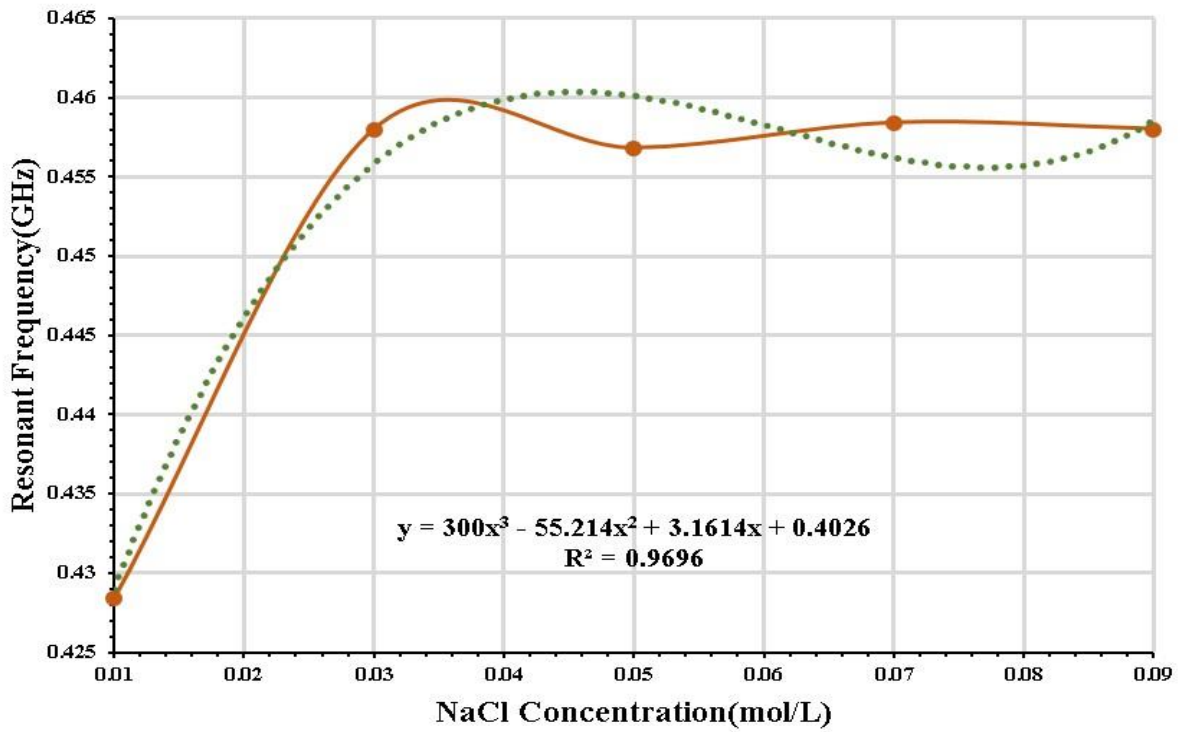


(a)

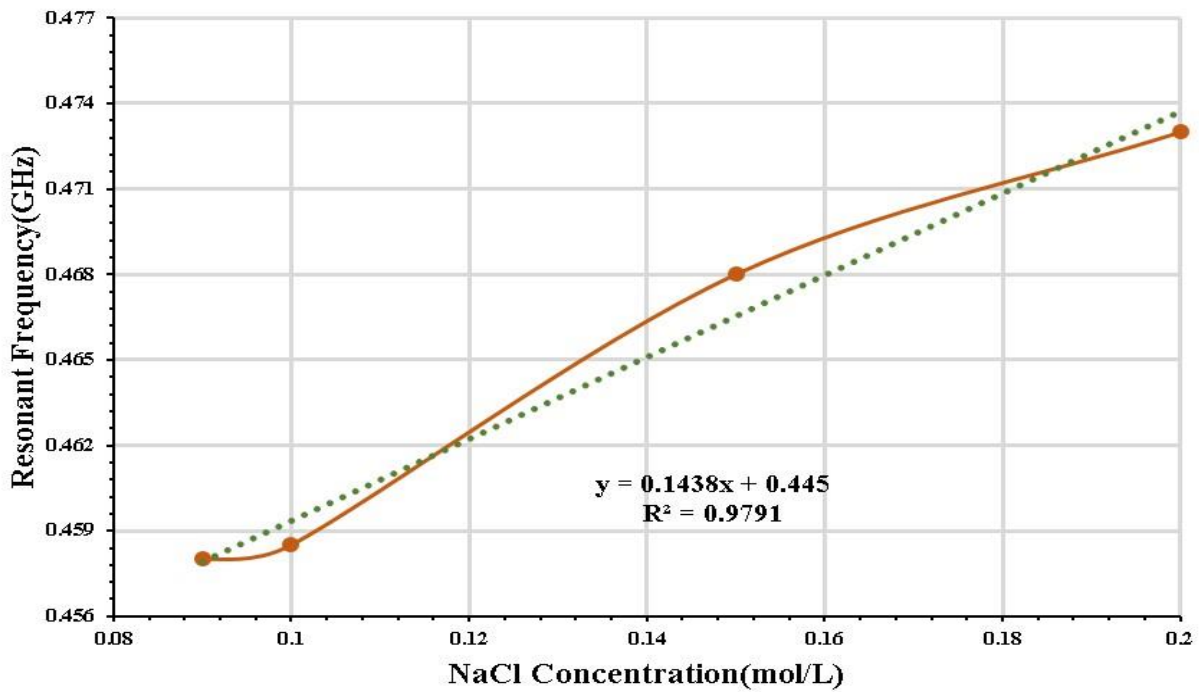


(b)

**Fig 4.6:** Frequency Vs Concentration for 10% increase antenna size (a) from 0.01 to 0.09 mol/L NaCl concentration (b) from 0.09 to 0.2 mol/L NaCl concentration.

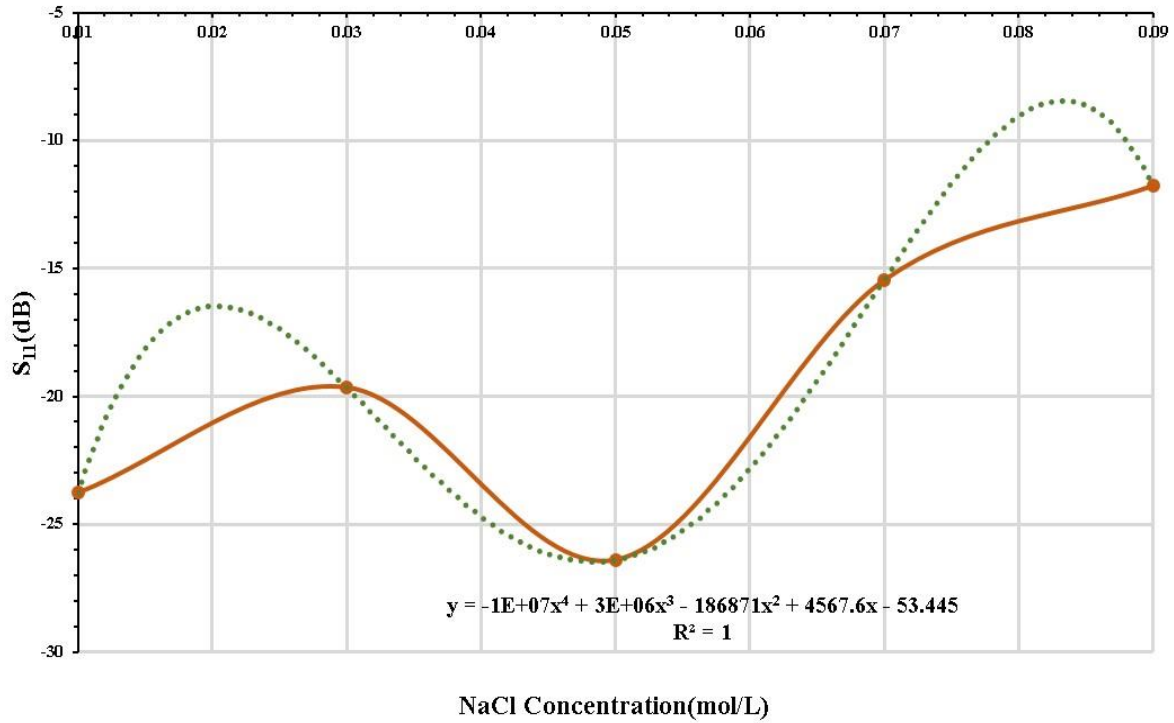


(a)

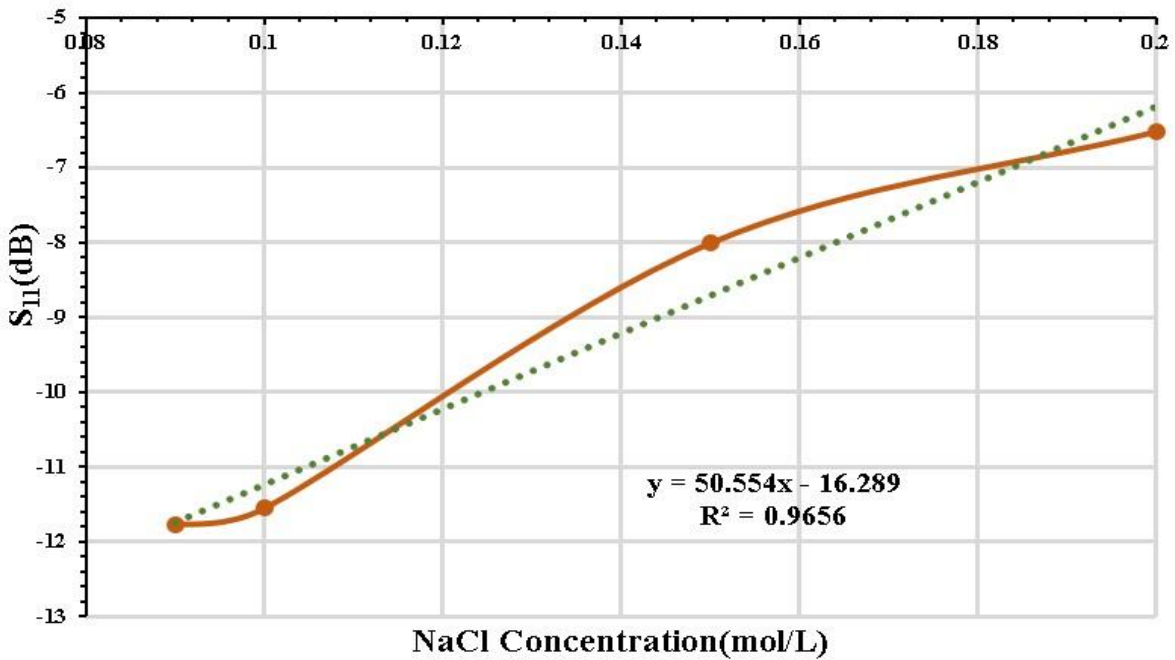


(b)

**Fig 4.7:** Frequency Vs Concentration for 20% increase antenna size (a) from 0.01 to 0.09 mol/L NaCl concentration (b) from 0.09 to 0.2 mol/L NaCl concentration.

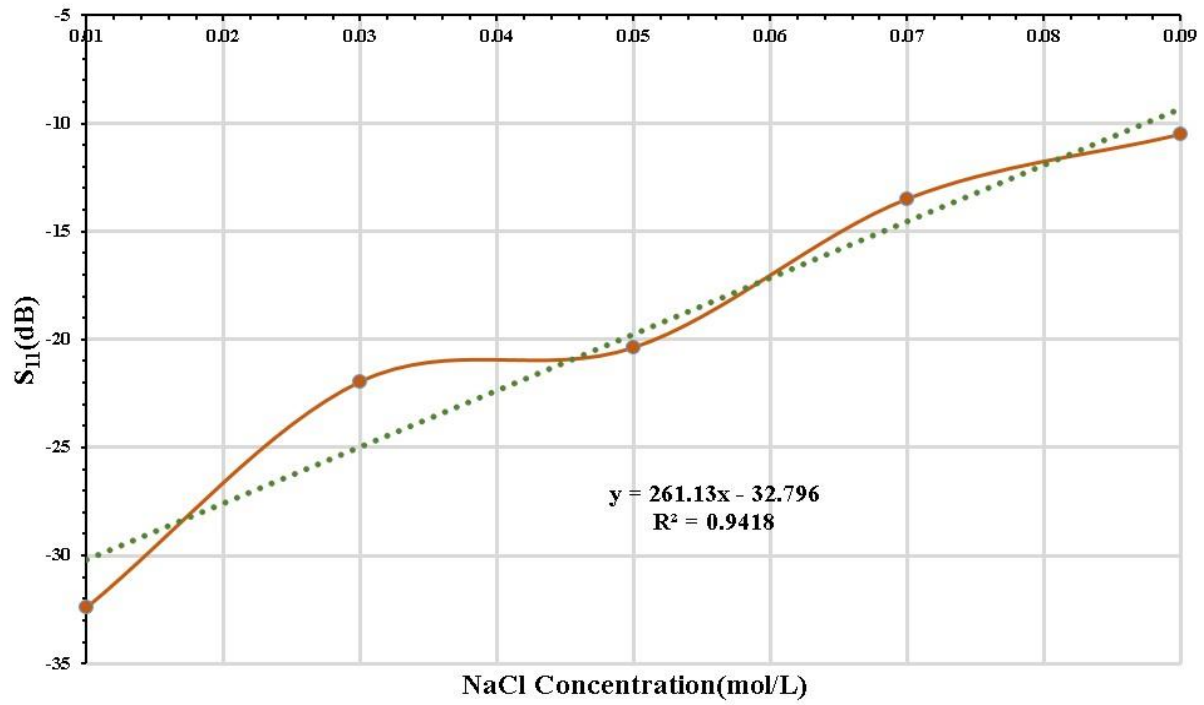


(a)

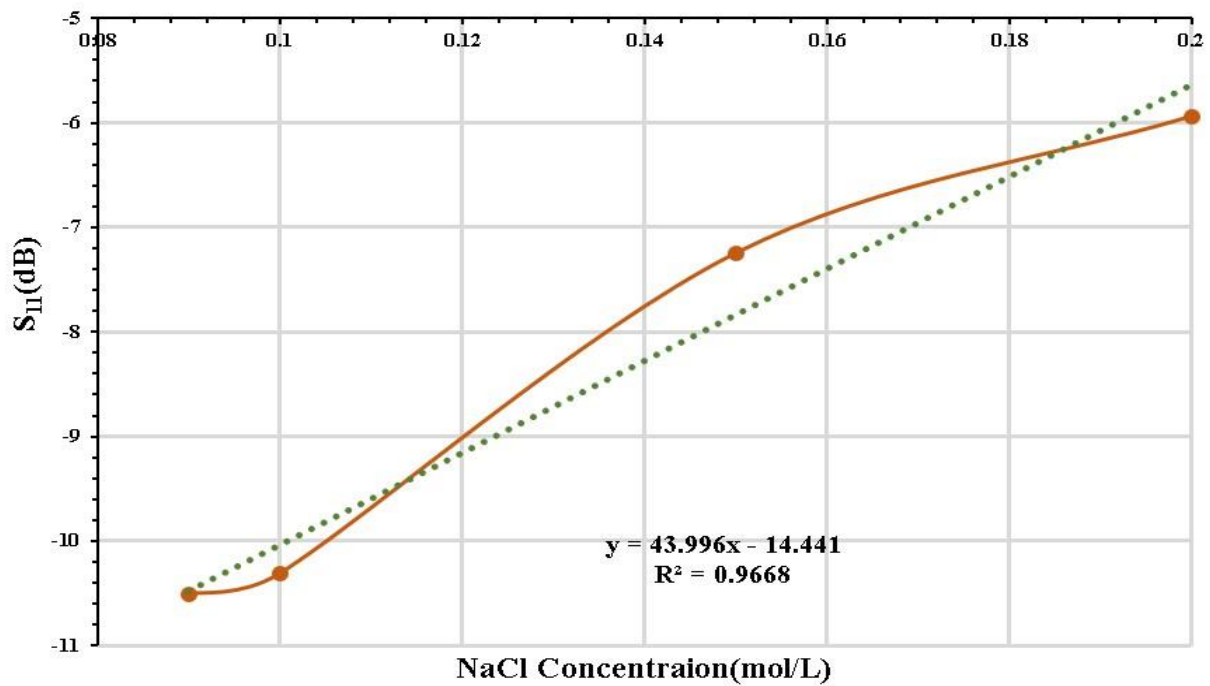


(b)

**Fig 4.8:**  $S_{11}$  Vs NaCl concentration 20% decrease antenna size (a) from 0.01 to 0.09 mol/L NaCl concentration (b) from 0.09 to 0.2 mol/L NaCl concentration.



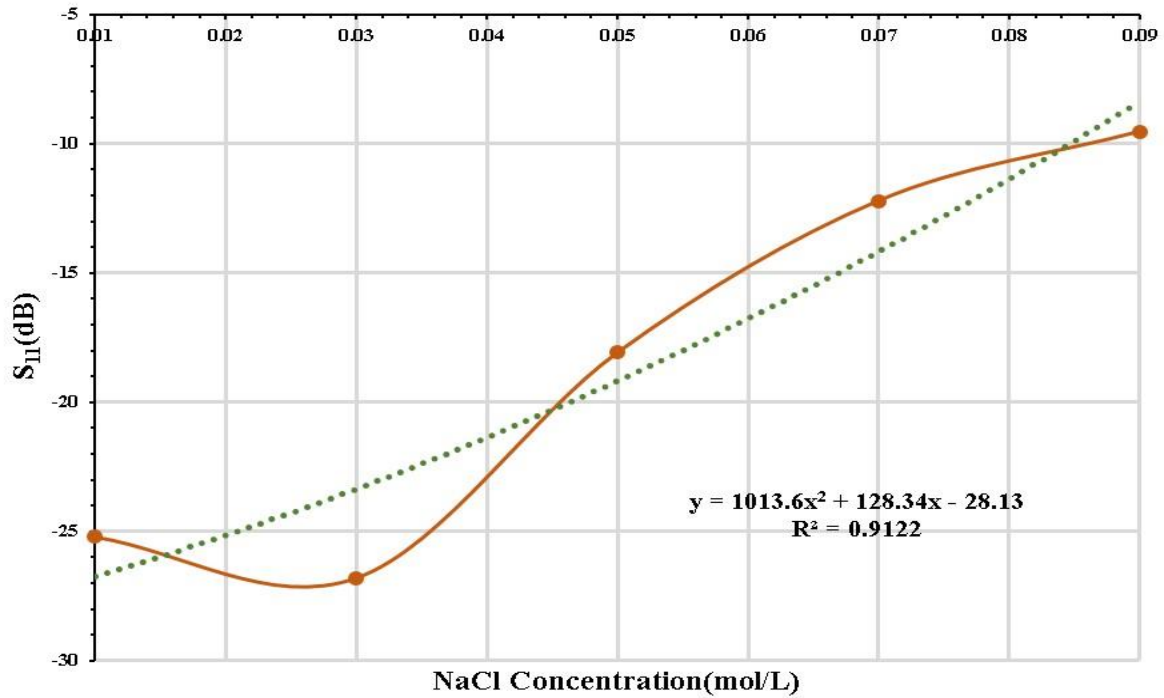
(a)



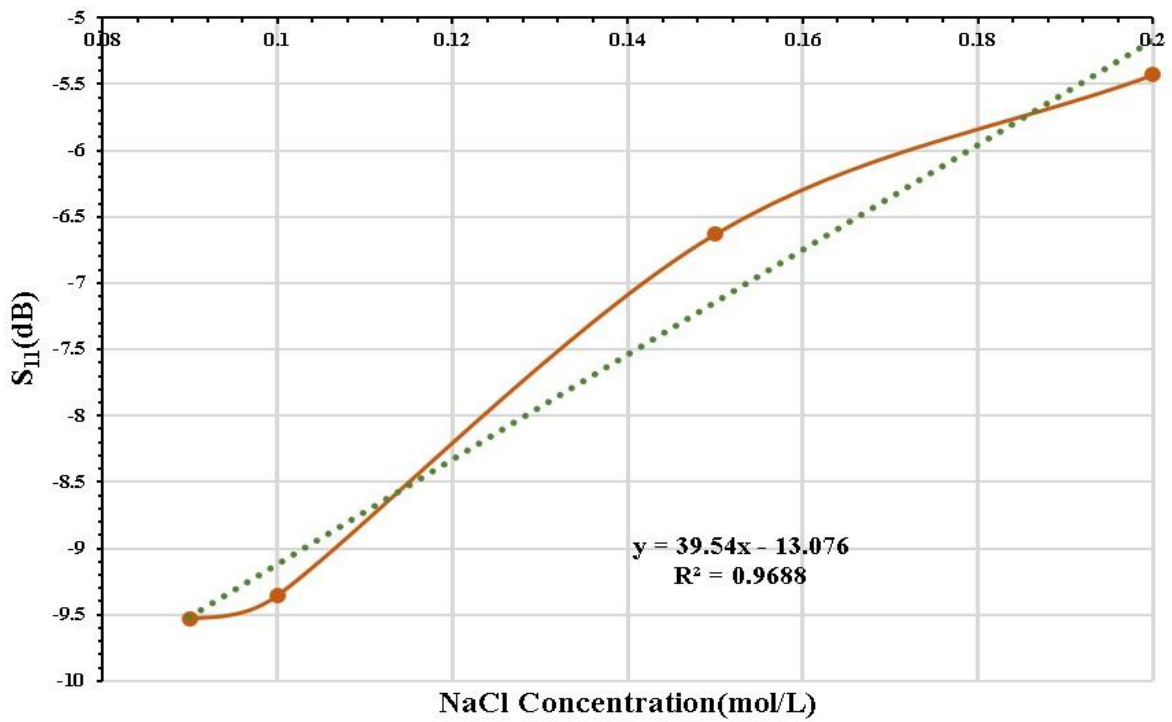
(b)

**Fig 4.9:**  $S_{11}$  Vs NaCl concentration 10% decrease antenna size (a) from 0.01 to 0.09 mol/L NaCl concentration (b) from 0.09 to 0.2 mol/L NaCl concentration.



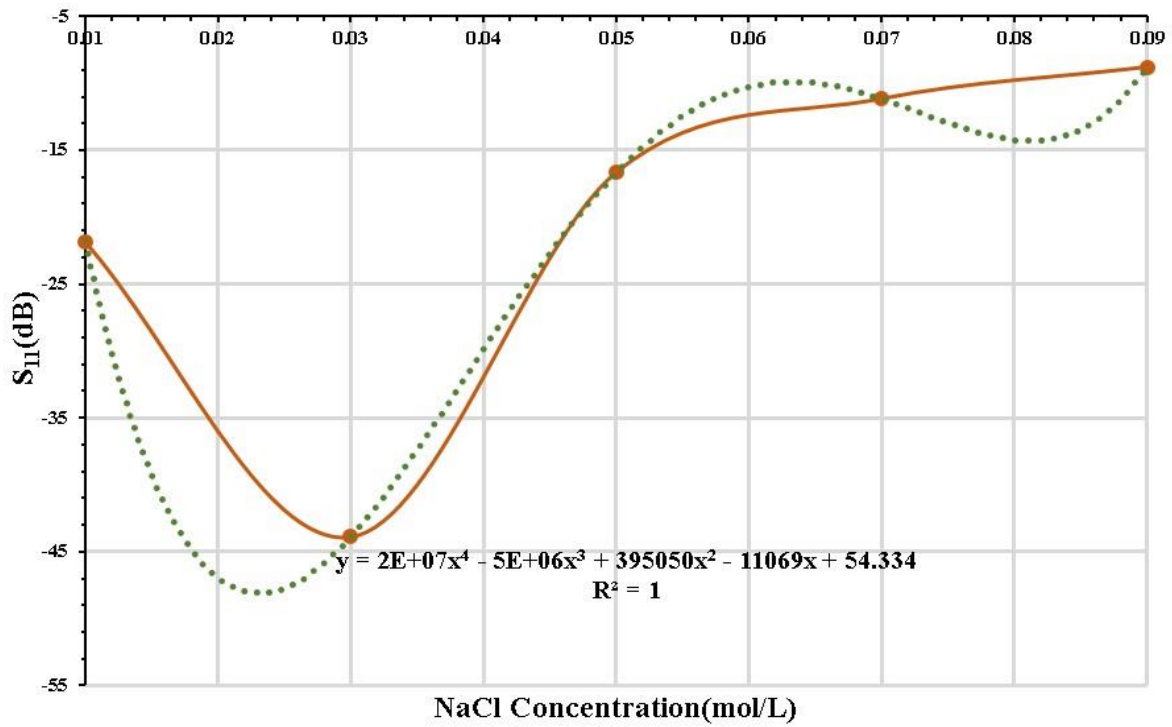


(a)

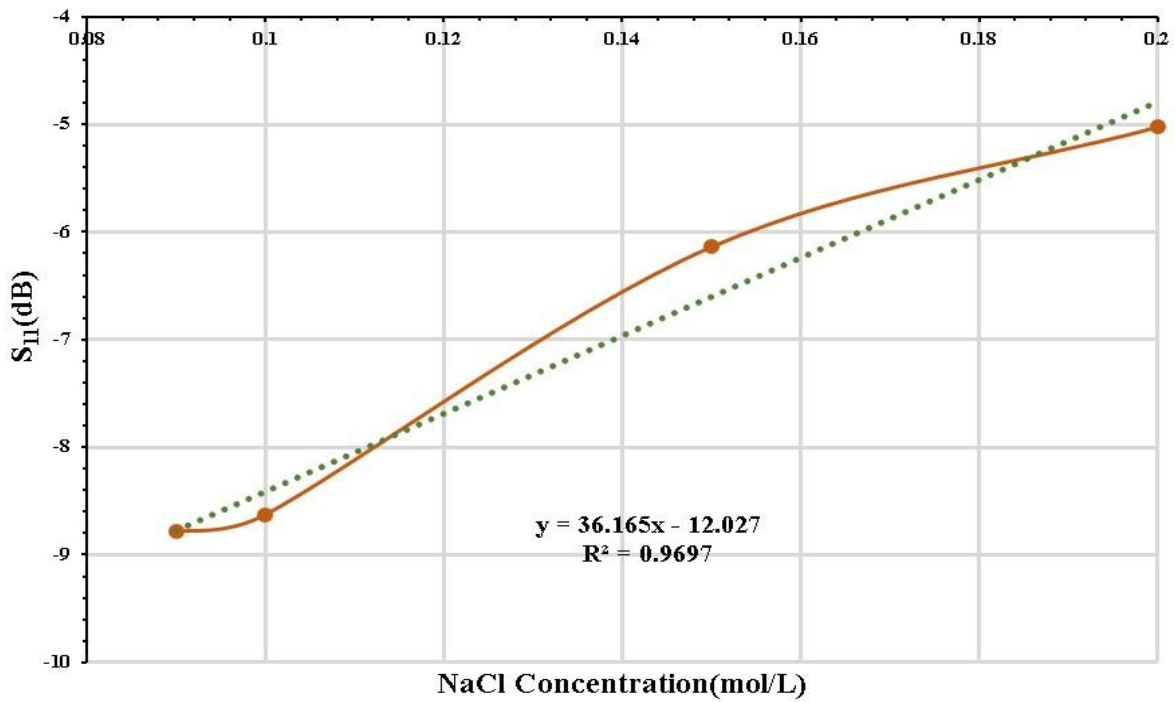


(b)

**Fig 4.10:**  $S_{11}$  Vs NaCl concentration actual antenna size (a) from 0.01 to 0.09 mol/L NaCl concentration (b) from 0.09 to 0.2 mol/L NaCl concentration.

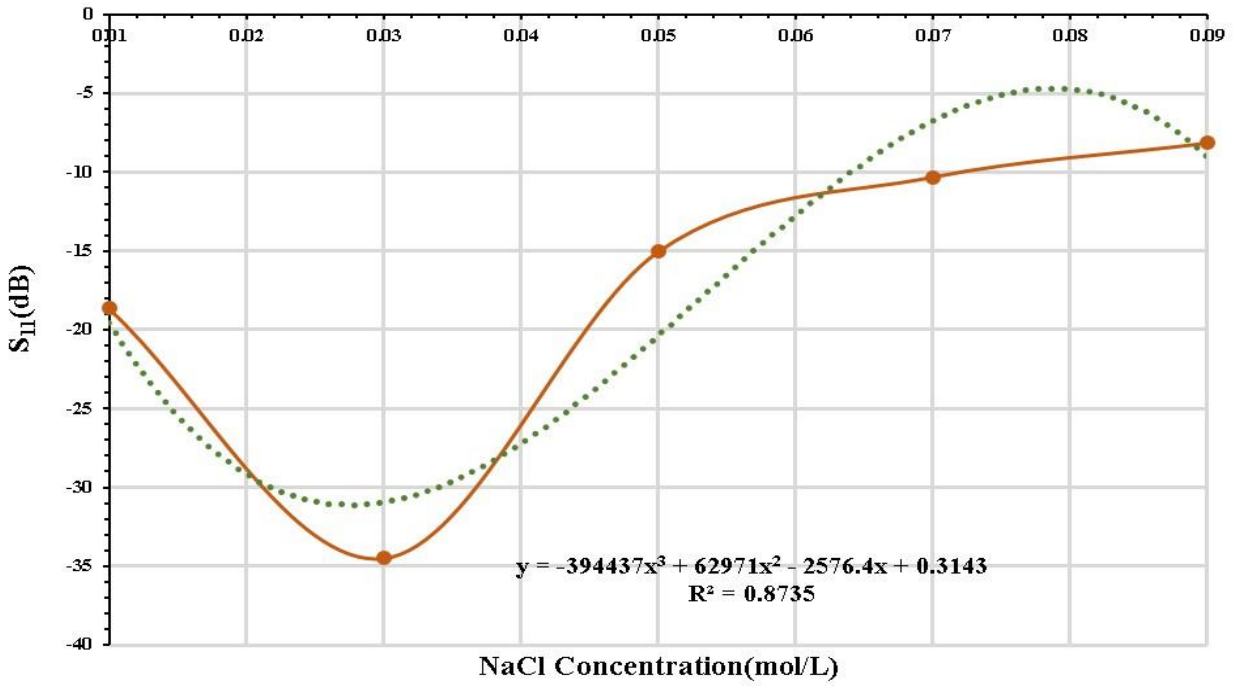


(a)

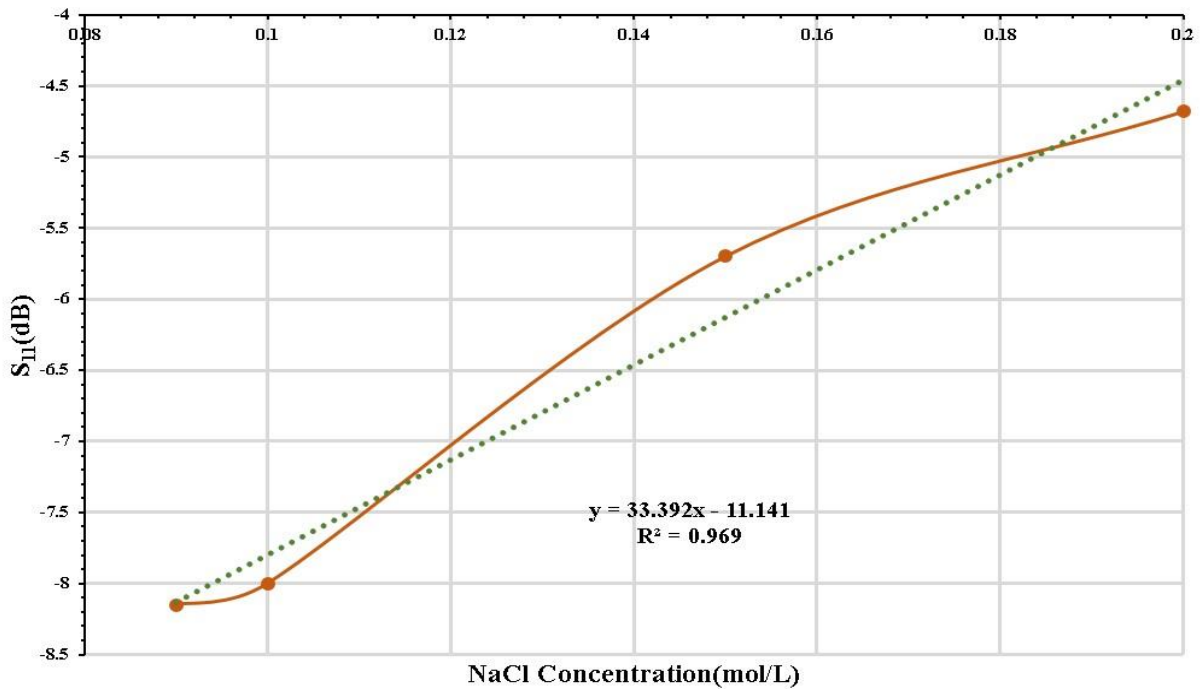


(b)

**Fig 4.11:**  $S_{11}$  Vs NaCl concentration 10% increase antenna size (a) from 0.01 to 0.09 mol/L NaCl concentration (b) from 0.09 to 0.2 mol/L NaCl concentration.



(a)



(b)

**Fig 4.12:**  $S_{11}$  Vs NaCl concentration 20% increase antenna size (a) from 0.01 to 0.09 mol/L NaCl concentration (b) from 0.09 to 0.2 mol/L NaCl concentration.

### 4.1.3 Error Calculation

From the software-driven results & equation-driven results there is a discrepancy. These errors can occur due to temperature changes because all the values of dielectric properties of NaCl solutions are taken based on room temperature. The following table will briefly show the errors for a particular concentration of NaCl solution.

Here we've taken 0.062 mol/L NaCl concentration as reference. The plot of  $S_{11}$  Vs resonant frequency for five different MPA-based sensor size is also shown below.

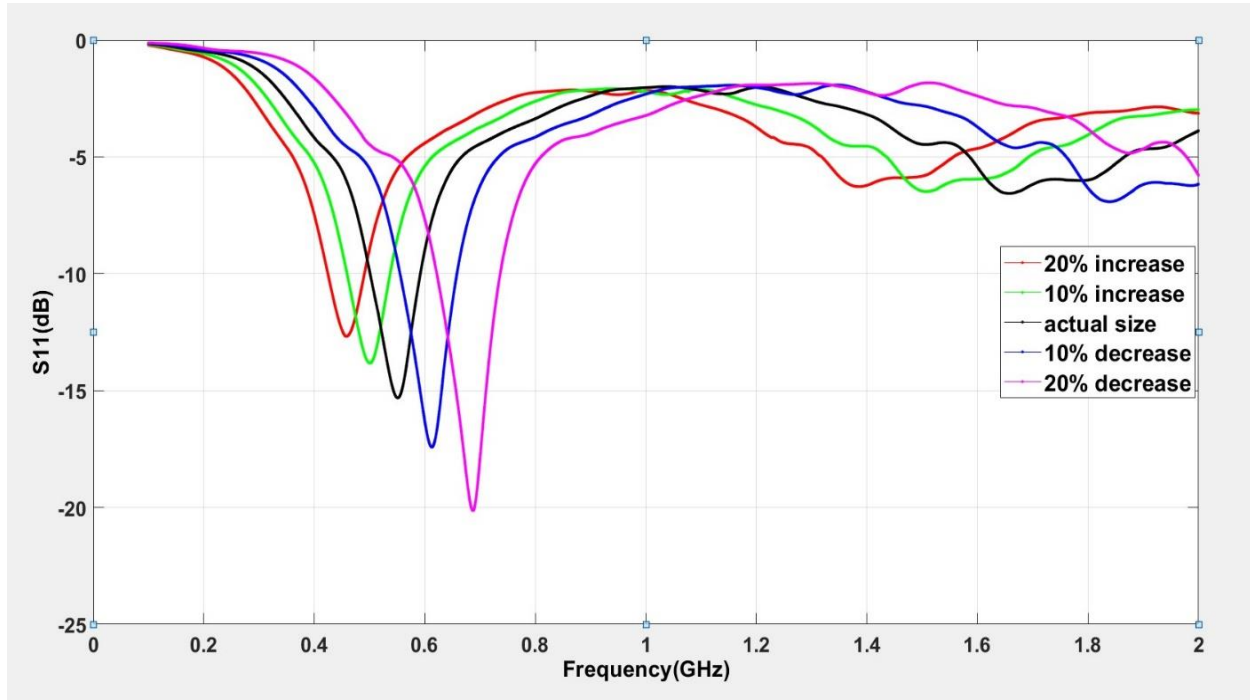


**Fig 4.13:**  $S_{11}$  Vs Resonant frequency plot for five different MPA-based sensor size having NaCl Concentration 0.062 mol/L

**Table 4.2:** Error chart for 0.062 mol/L concentration of NaCl solution (Total size variation)

Antenna Size	Error percentage ( $S_{11}$ vs. conc)	Error percentage (Freq vs. conc)
20% decrease	1.14	0.29
10% decrease	4.66	0.13
Actual Size	6.28	0.177
10% increase	3.79	0.178
20% increase	10.35	0.03

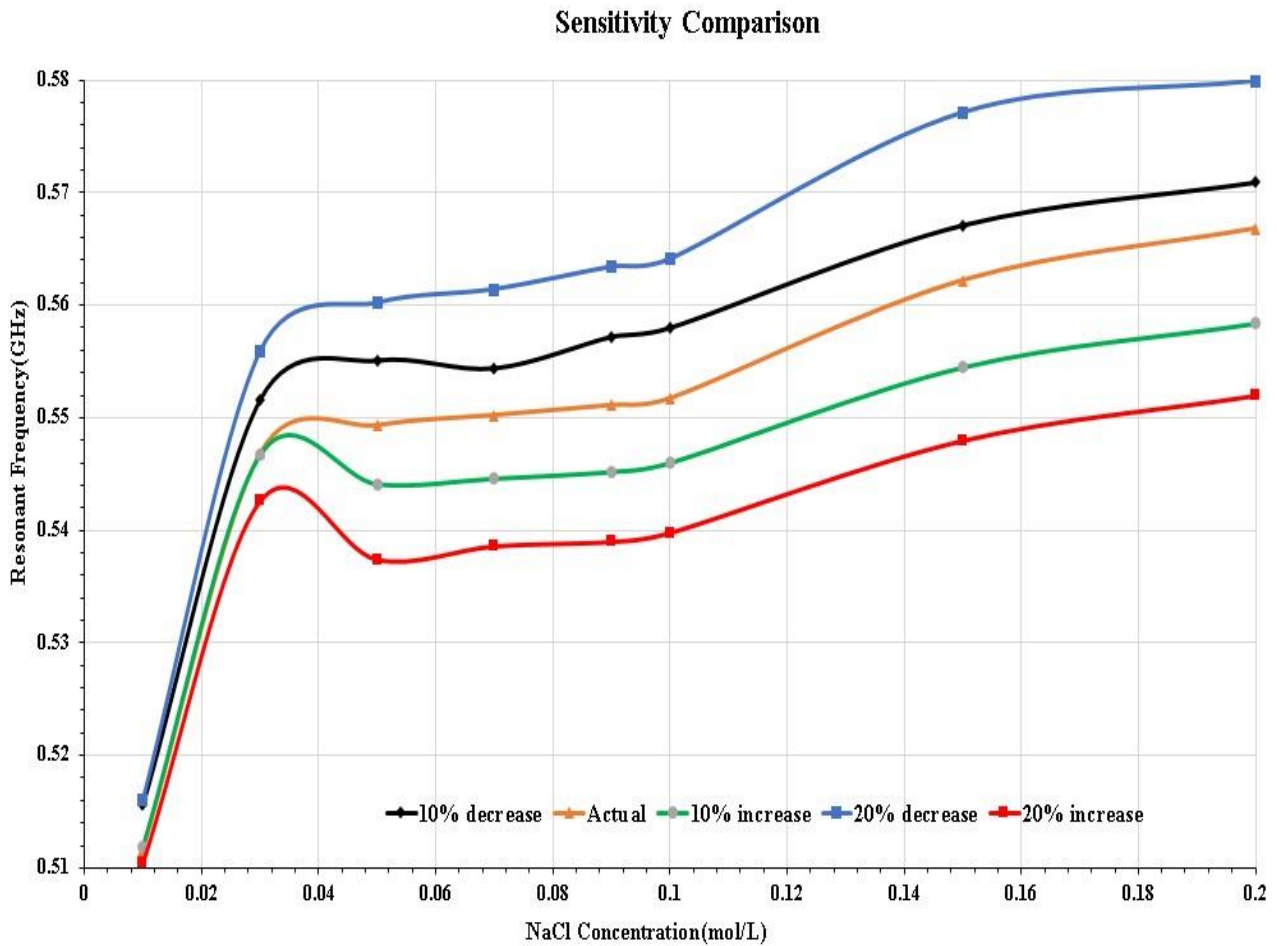
## 4.2 Feed line width variation of MPA-based sensor

A small change in the design of the antenna can vary the result in a different manner. The original feed line width of the antenna was 3.2 mm. By decreasing and increasing the value of the width of the feed-line, changes can be obtained which are shown in the following part.

### 4.2.1 Sensitivity

Figures 4.1 and 4.2 delineate the resonant frequency and reflection coefficient (S11) of the sensor regarding NaCl concentration in sweat separately. It was examined that there was a huge change in the reflection coefficient and resonant frequency of the sensor because of the variety in NaCl concentration for various sensor sizes. The direct relapse examination was applied to the deliberate information and a decent relationship was seen between the s-parameter and NaCl concentrations.

**Fig 4.14:** Resonant frequency vs NaCl concentration curve for five different MPA-based sensor size by varying feed line.



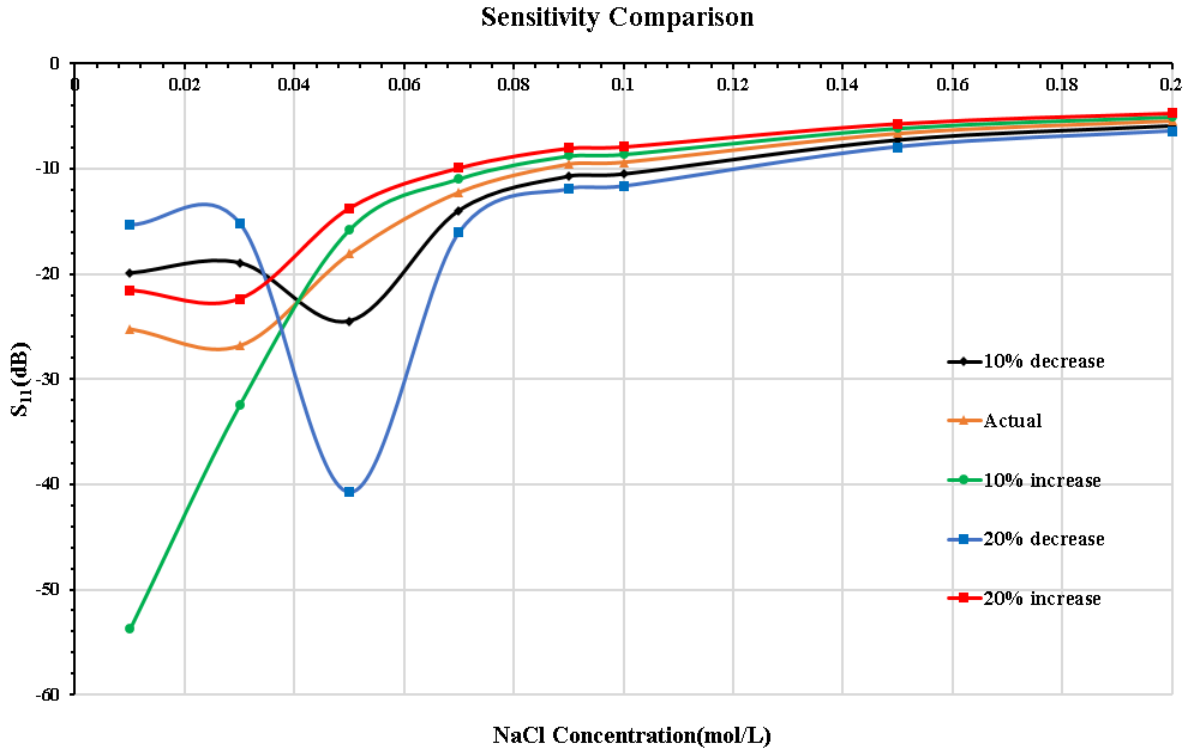


**Fig 4.15:** Reflection co-efficient( $s_{11}$ ) vs NaCl concentration curve for five different MPA-based sensor sizes by varying feed line.

As before, for summarizing the fact a table is given below regarding reflection parameters, resonant frequency, NaCl solution concentration for various antenna sizes for proposed antenna. It tends to be noticed obviously from the slope changes because of frequency & reflection co-efficient shifting, the sensor was able to display the adjustment of its reflection properties with NaCl concentration with variations in antenna size.

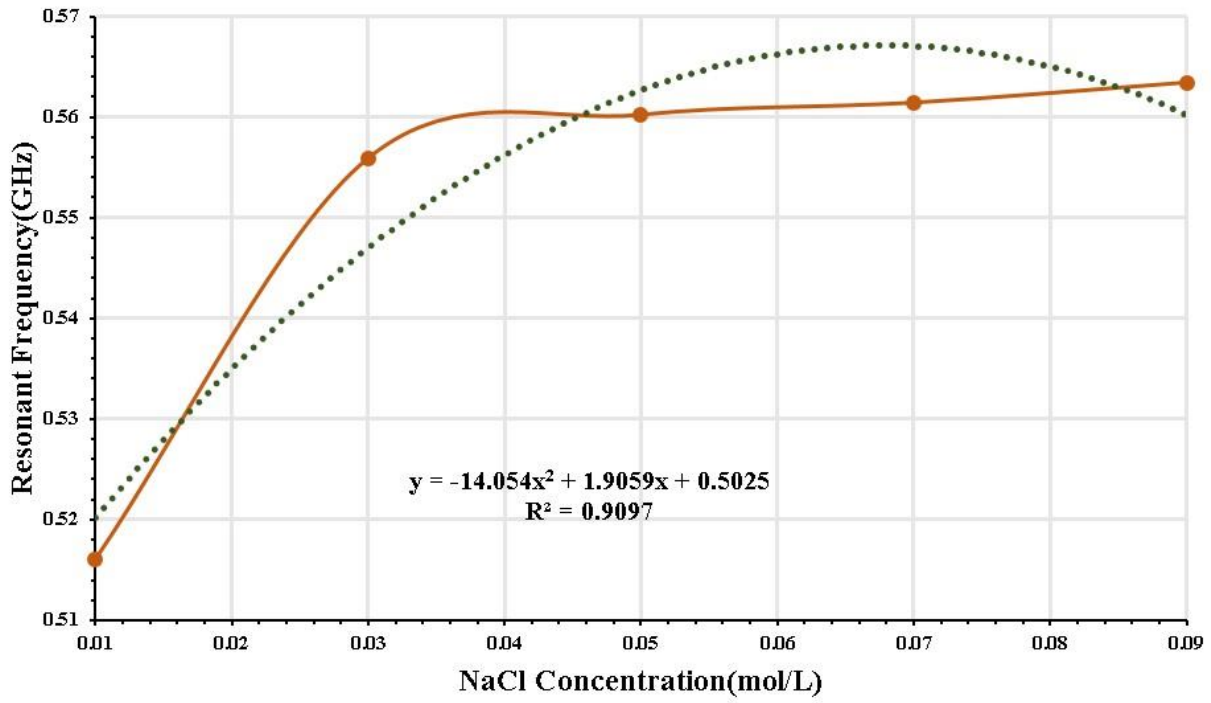
**Table 4.3:** Sensitivity Table (Feed line width variation)

SI No.	Parameters	Concentration (mol/L)	Frequency (GHz)	$S_{11}$ Parameter(dB)	Sensitivity Slope (in terms of freq shift)	Sensitivity Slope (in terms of $S_{11}$ shift)
1.	20% decrease	0.01	0.5161	-15.3681	0.2513	119.926
		0.03	0.5559	-15.2233		
		0.05	0.5602	-40.7475		
		0.07	0.5614	-16.0651		
		0.09	0.5634	-11.9402		
		0.1	0.5641	-11.684		
		0.15	0.5771	-7.94997		
		0.2	0.5799	-6.44951		

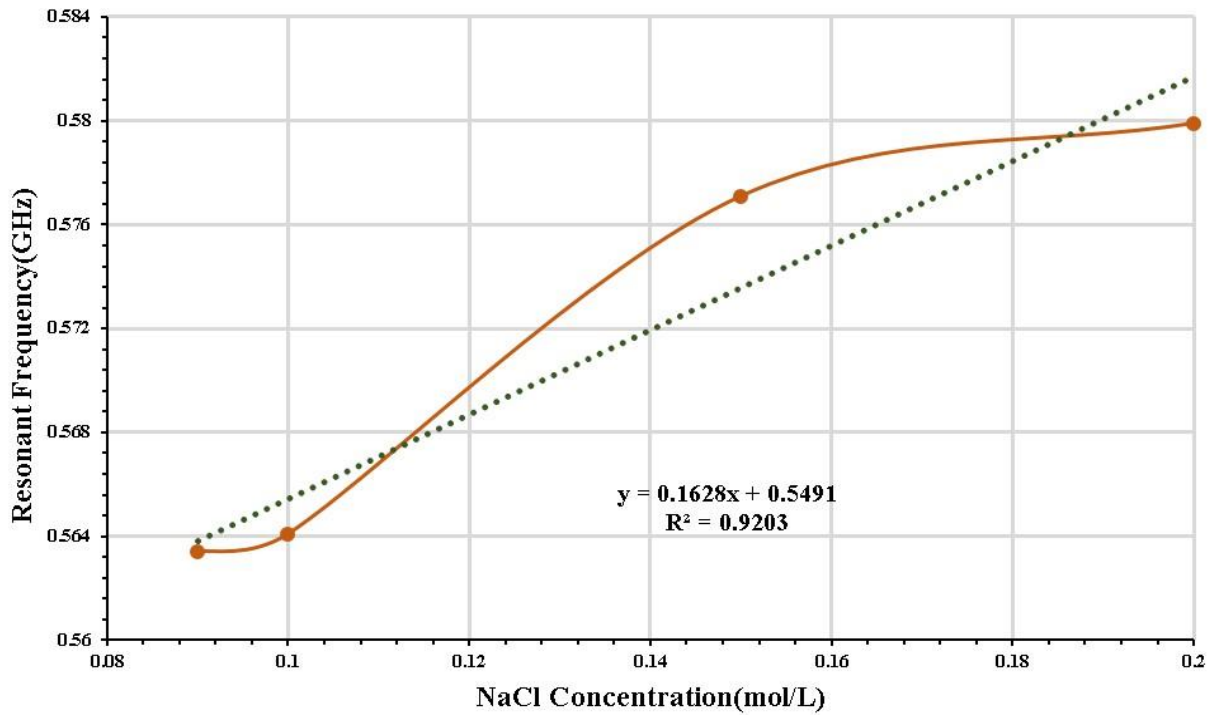
2.	10% decrease	0.01	0.5156	-19.9199	0.2106	95.124
		0.03	0.5516	-18.9399		
		0.05	0.5551	-24.4711		
		0.07	0.5544	-13.9596		
		0.09	0.5572	-10.7216		
		0.1	0.558	-10.5086		
		0.15	0.5671	-7.27932		
		0.2	0.5709	-5.93479		
3.	Actual Size	0.01	0.5116	-25.214	0.2111	107.325
		0.03	0.5468	-26.796		
		0.05	0.5493	-18.082		
		0.07	0.5502	-12.214		
		0.09	0.5511	-9.535		
		0.1	0.5517	-9.36		
		0.15	0.5622	-6.631		
		0.2	0.5668	-5.427		
4.	10% increase	0.01	0.5119	-53.7499	0.1666	121.625
		0.03	0.5467	-32.4522		
		0.05	0.5441	-15.774		
		0.07	0.5446	-10.933		
		0.09	0.5452	-8.754		
		0.1	0.546	-8.600		
		0.15	0.5545	-6.128		
		0.2	0.5584	-5.04		
5.	20% increase	.01	0.5104	-21.5303	0.1482	84.847
		.03	0.5426	-22.3587		
		.05	0.5374	-13.7306		
		.07	0.5386	-9.90518		
		.09	0.539	-8.02839		
		.10	0.5398	-7.89467		
		.15	0.548	-5.68802		
		.20	0.552	-4.69274		

#### 4.2.2 Linearity (Feedline width variation)

For the linearity property calculation for different feed-line width sizes, we've used two kinds of graphs which are Resonant frequency vs. concentration and  $S_{11}$  vs. concentration. After that, the error is calculated between the results obtained from the software and the results obtained from the equations.



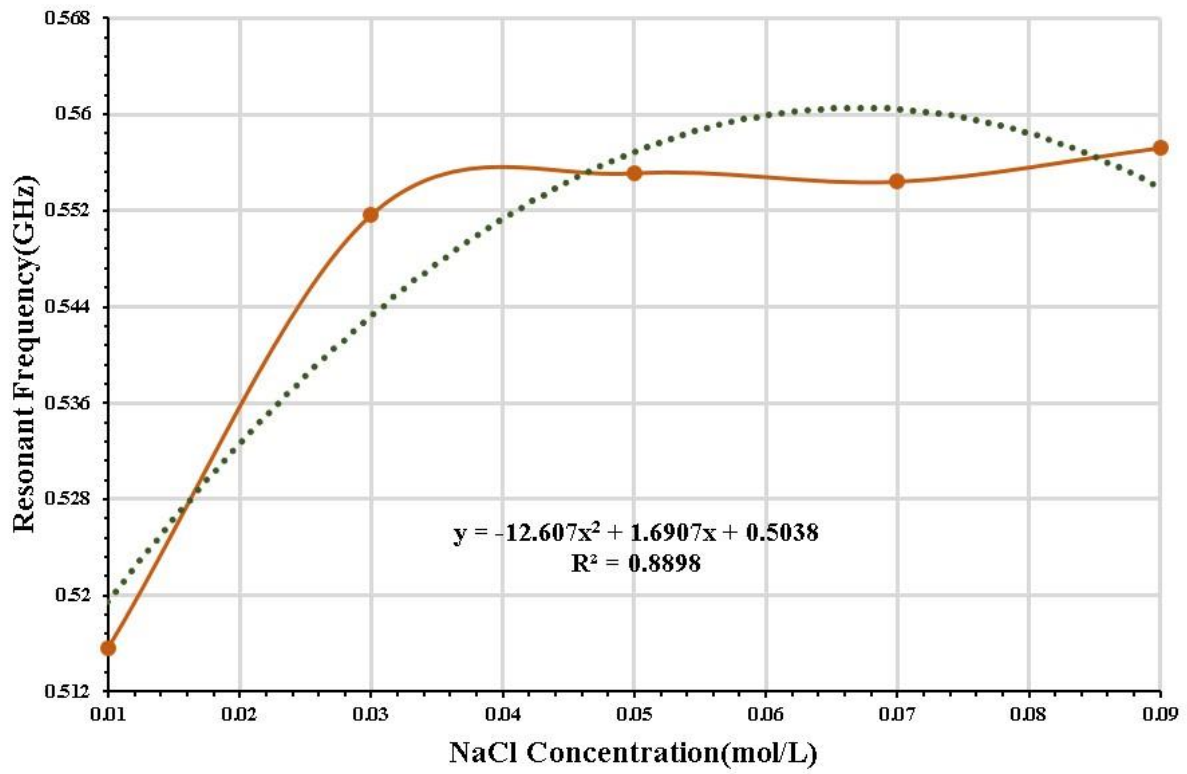
(a)



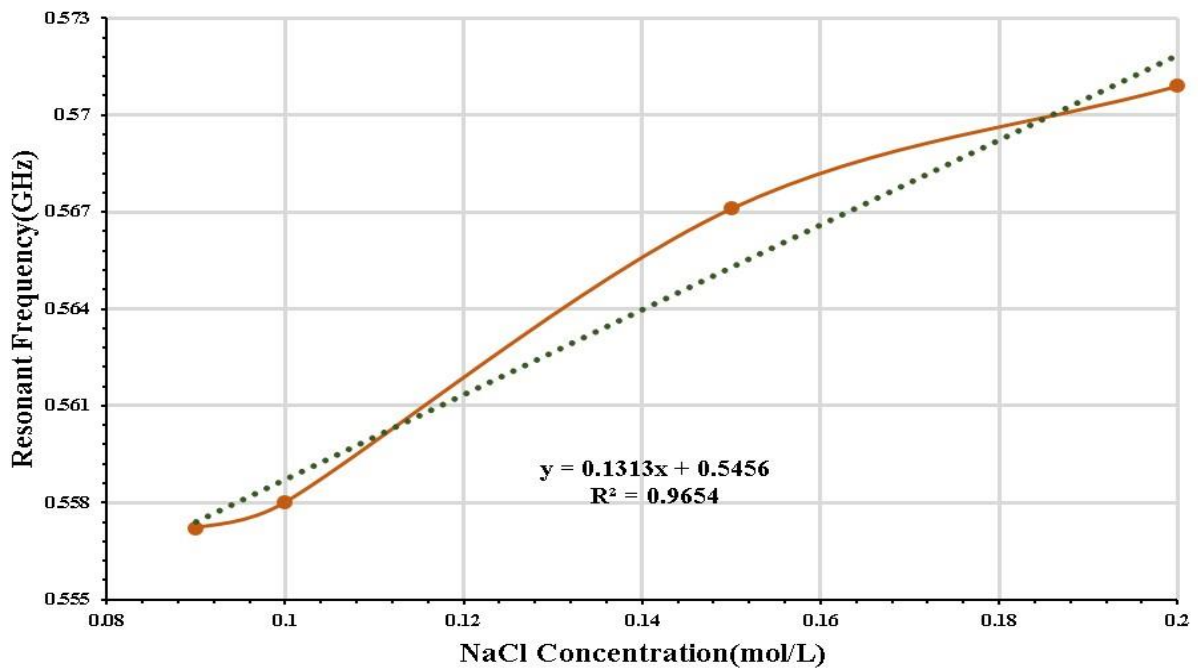
(b)

**Fig 4.16:** Frequency Vs Concentration for 20% decrease antenna size by varying feedline (a) from 0.01 to 0.09 mol/L NaCl concentration (b) from 0.09 to 0.2 mol/L NaCl concentration.



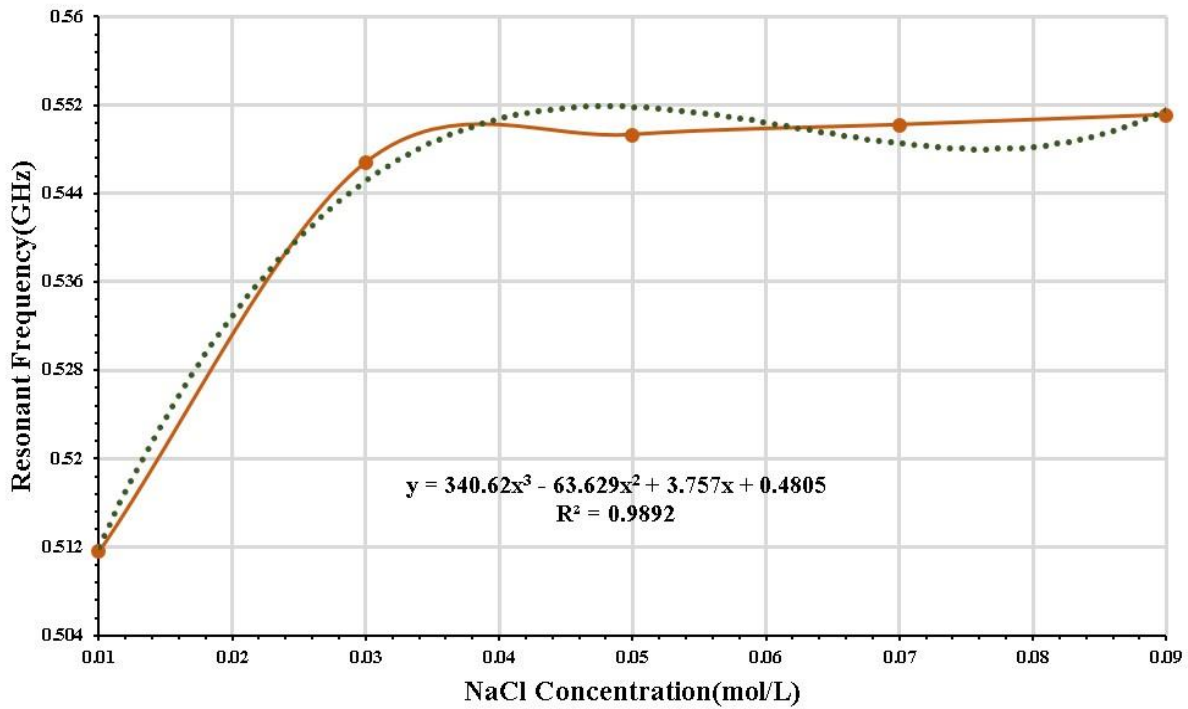


(a)

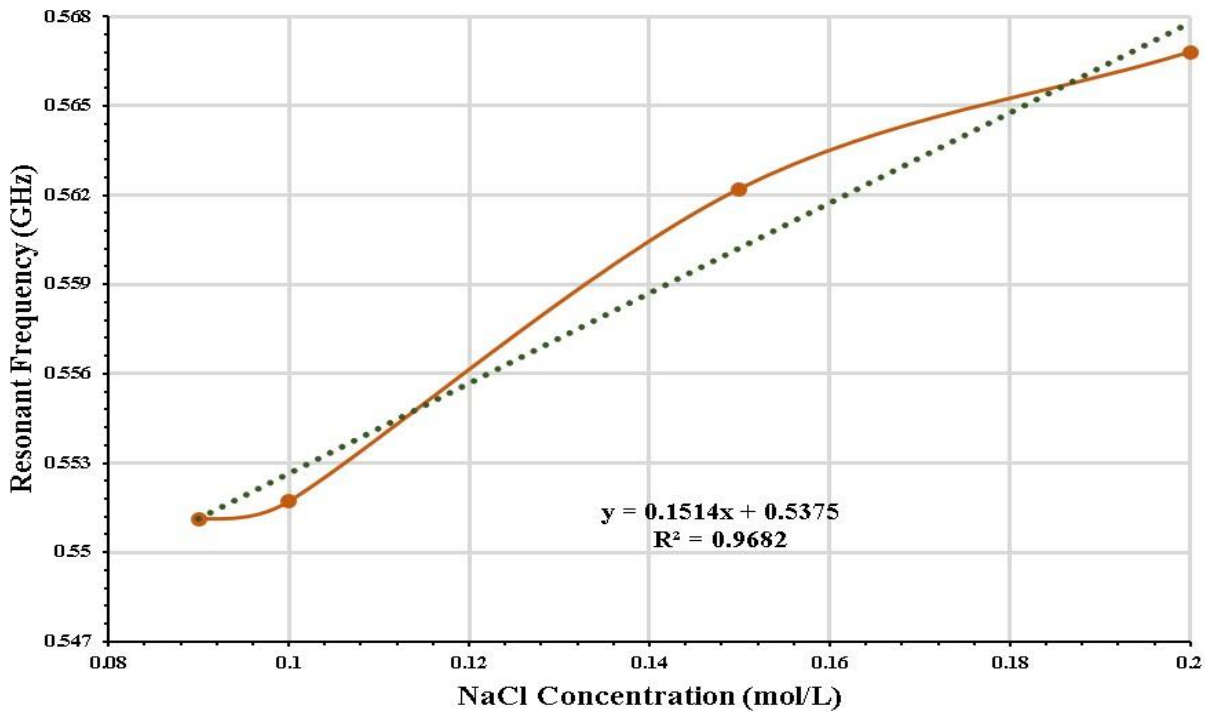


(b)

**Fig 4.17:** Frequency Vs Concentration for 10% decrease antenna size by varying feedline (a) from 0.01 to 0.09 mol/L NaCl concentration (b) from 0.09 to 0.2 mol/L NaCl concentration.

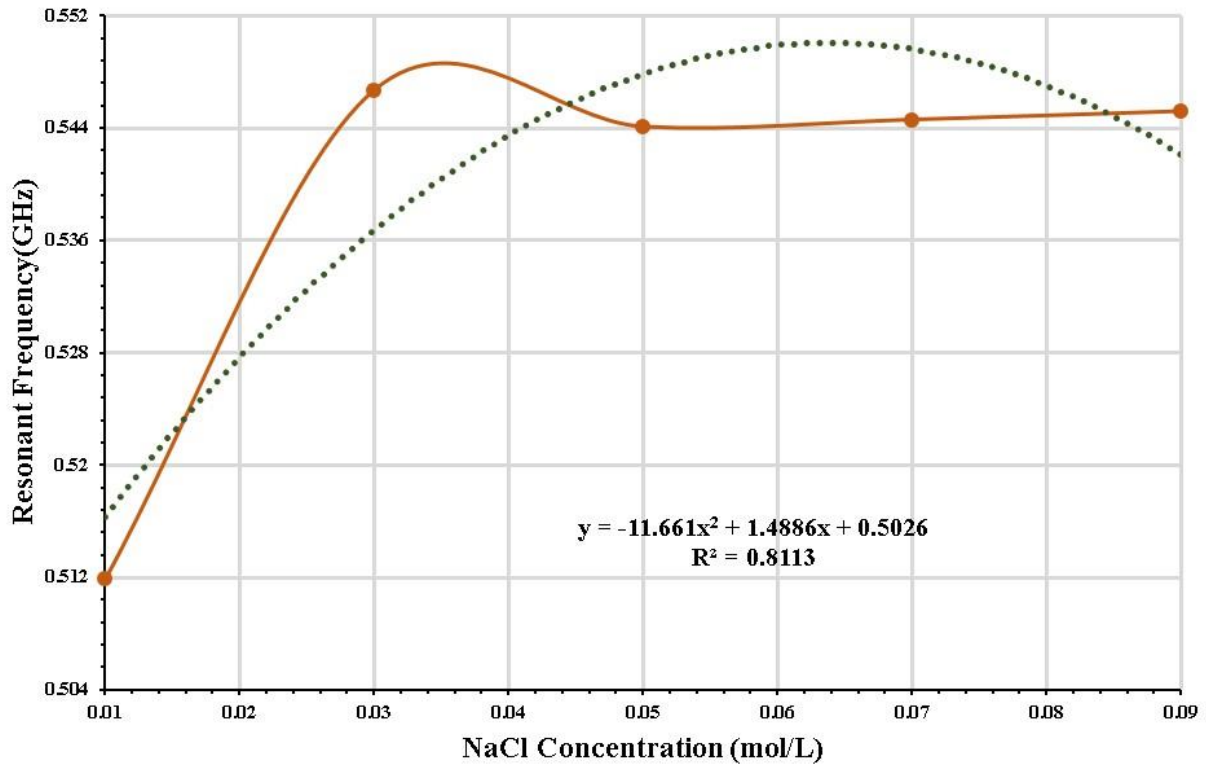


(a)

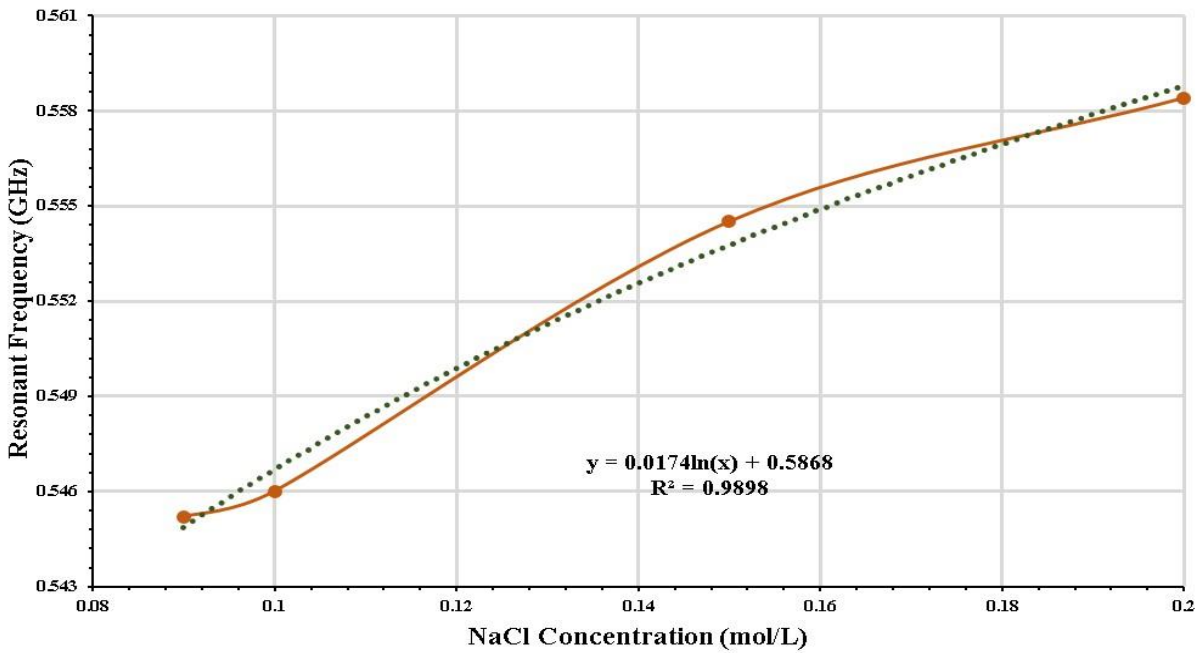


(b)

**Fig 4.18:** Frequency Vs Concentration for actual antenna size by varying feedline (a) from 0.01 to 0.09 mol/L NaCl concentration (b) from 0.09 to 0.2 mol/L NaCl concentration.

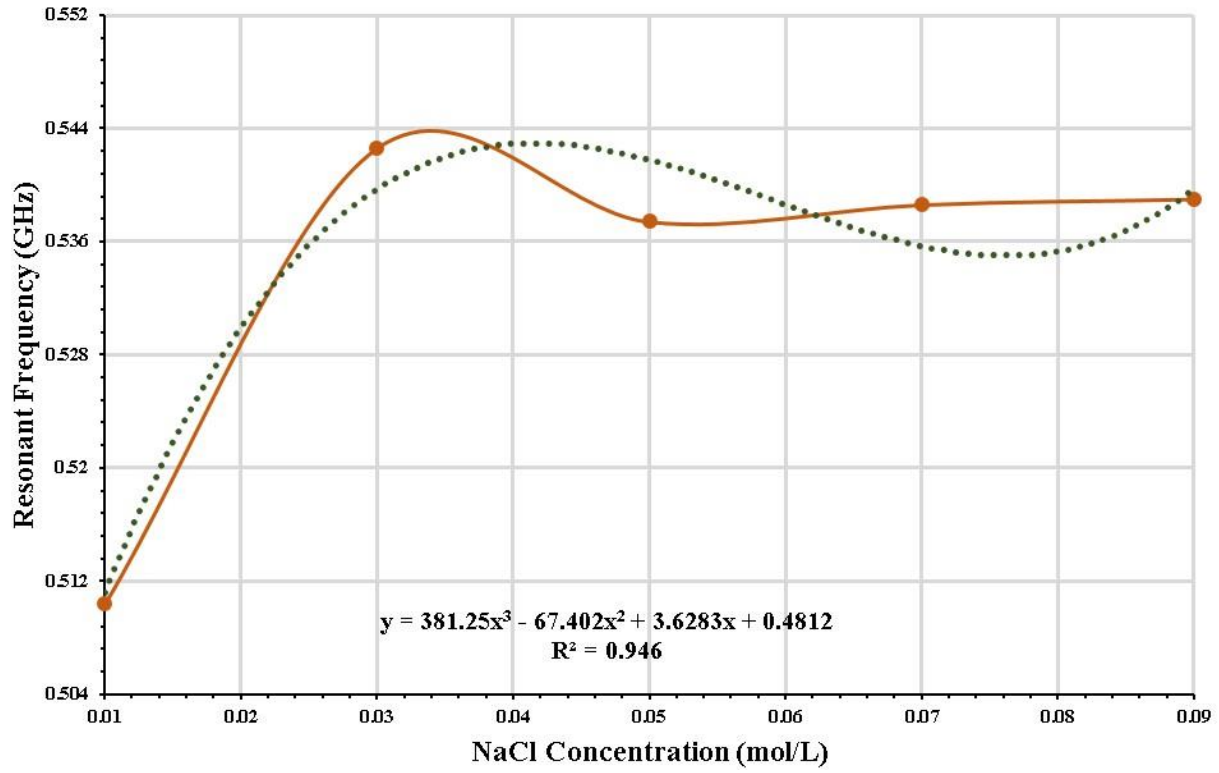


(a)

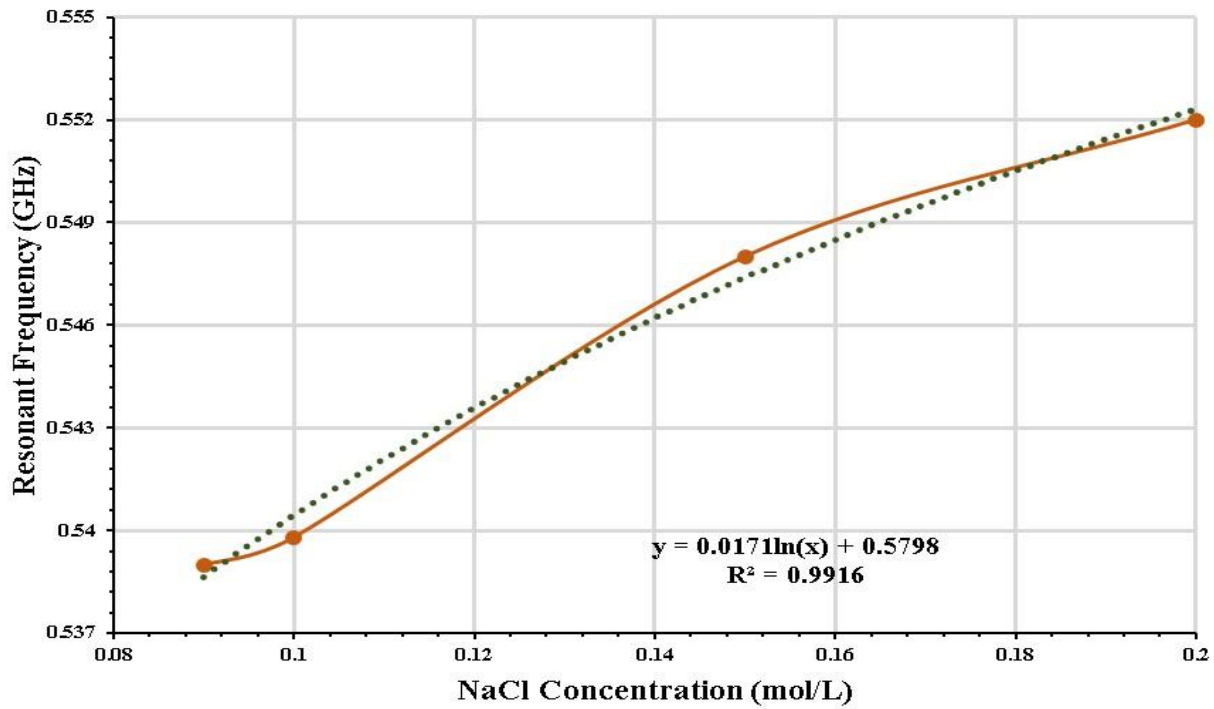


(b)

**Fig 4.19:** Frequency Vs Concentration for 10% increase antenna size by varying feedline (a) from 0.01 to 0.09 mol/L NaCl concentration (b) from 0.09 to 0.2 mol/L NaCl concentration.

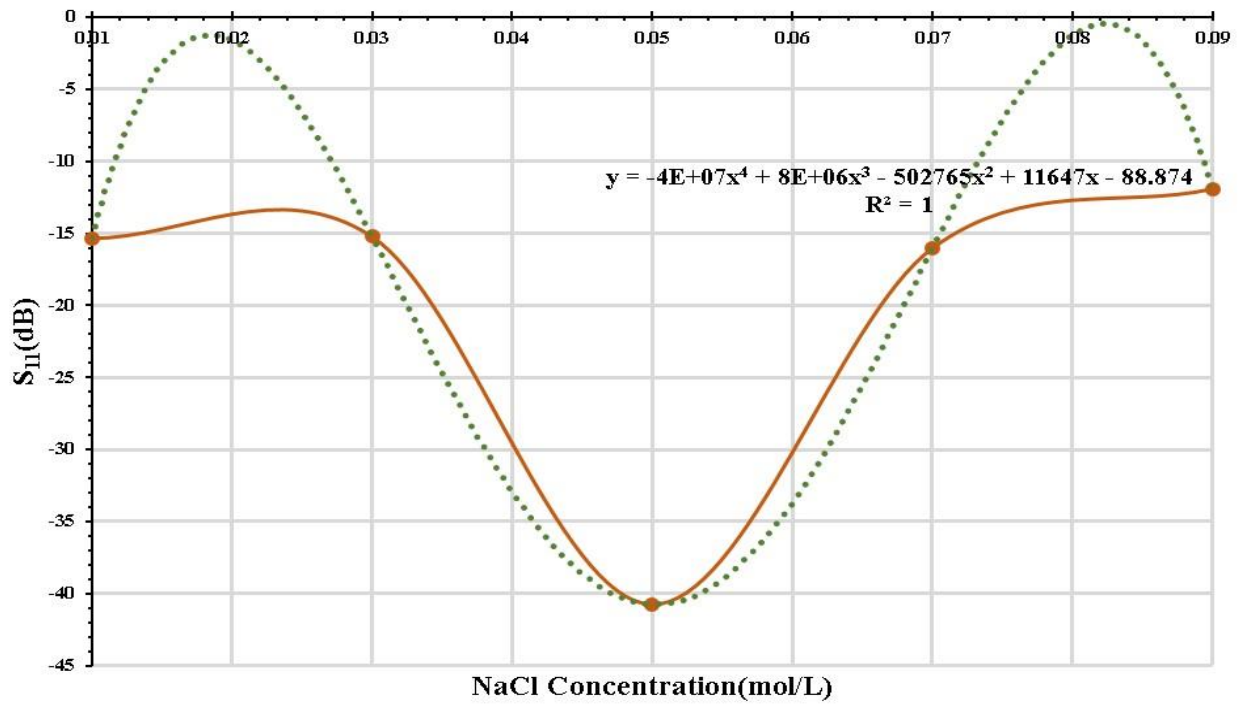


(a)

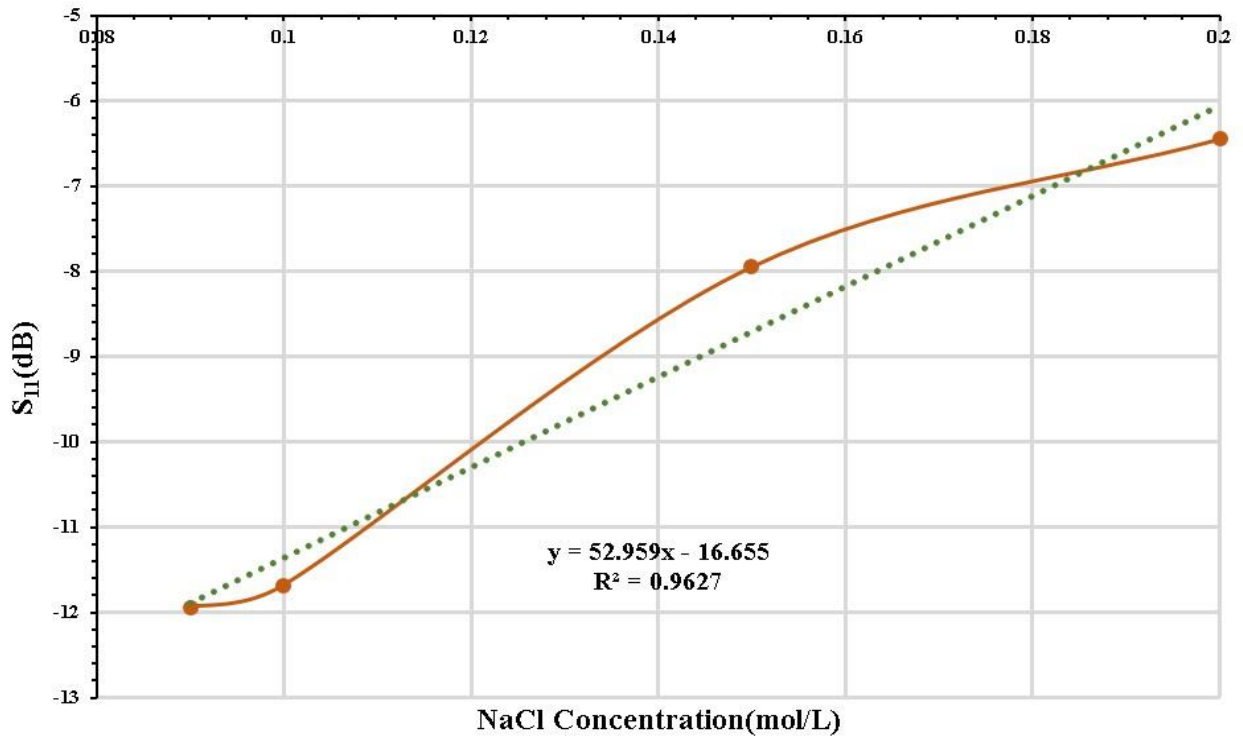


(b)

**Fig 4.20:** Frequency Vs Concentration for 20% increase antenna size by varying feedline (a) from 0.01 to 0.09 mol/L NaCl concentration (b) from 0.09 to 0.2 mol/L NaCl concentration.

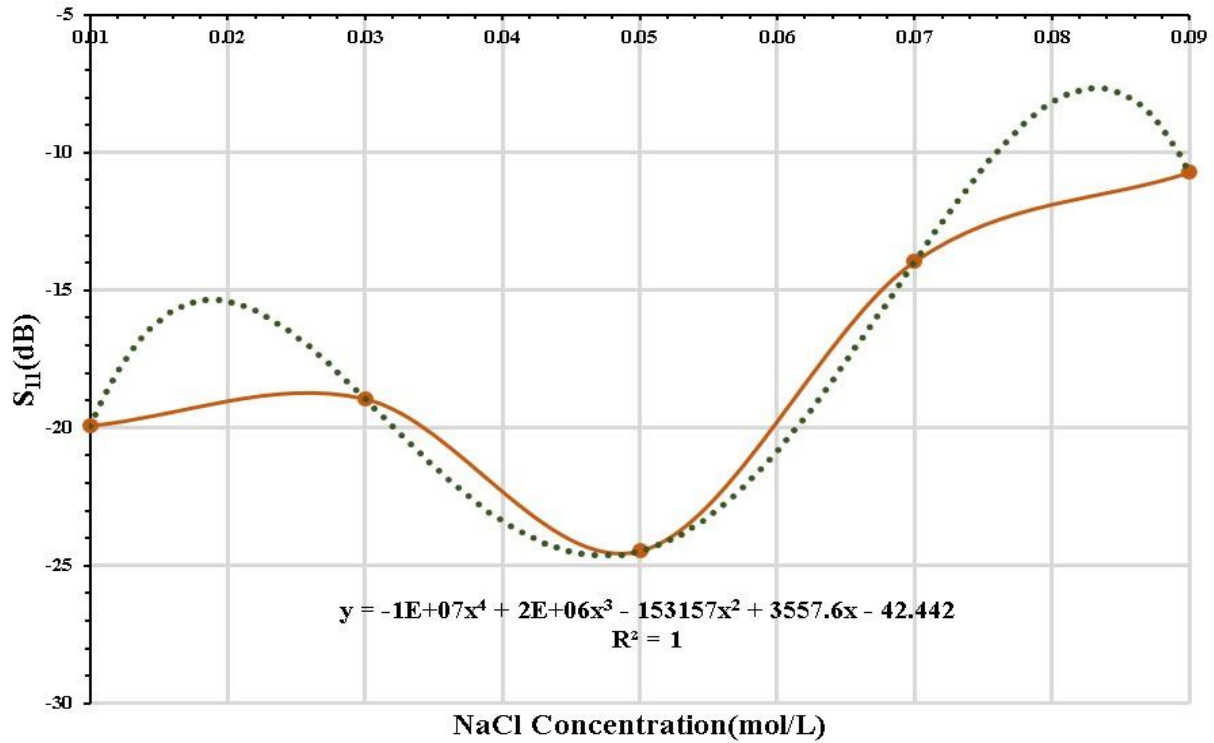


(a)



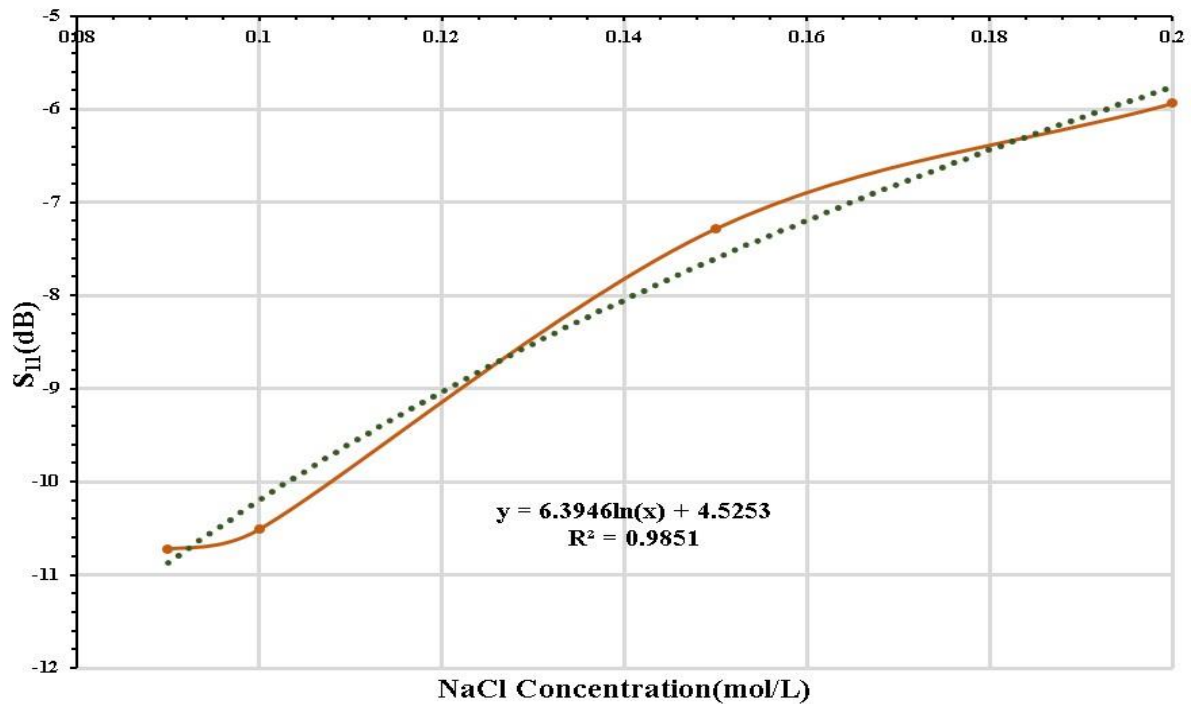
(b)

**Fig 4.21:**  $S_{11}$  Vs Concentration for 20% decrease antenna size by varying feedline (a) from 0.01



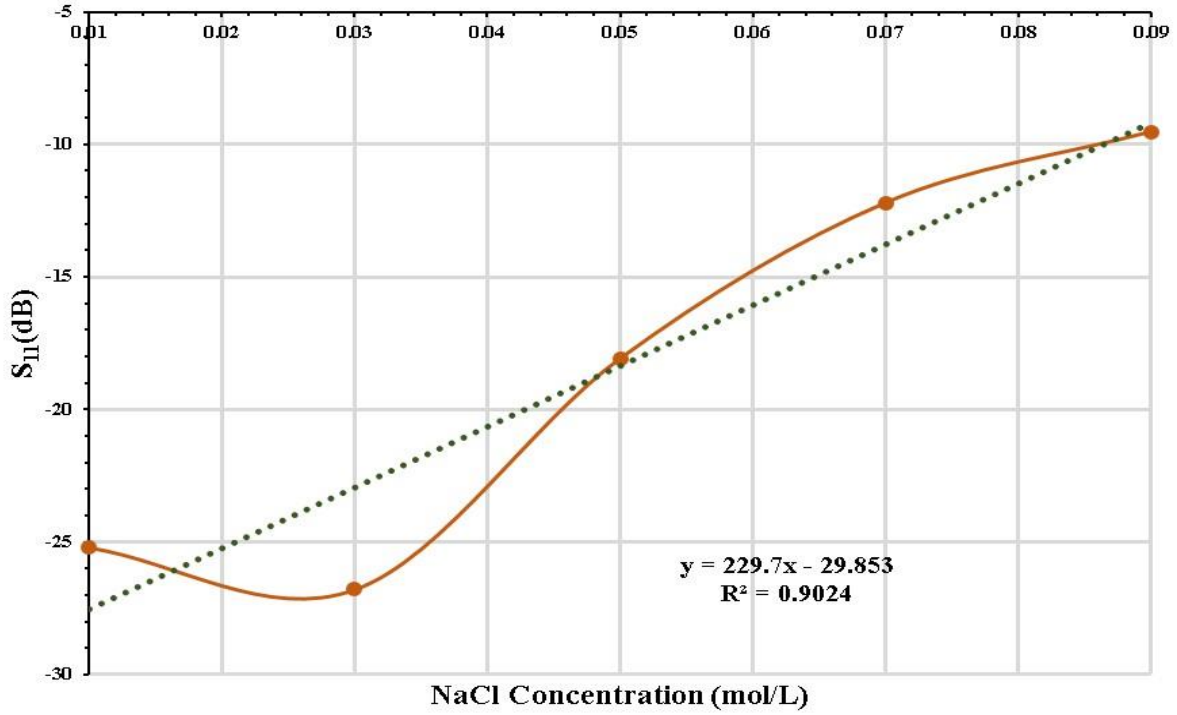
to 0.09 mol/L NaCl concentration (b) from 0.09 to 0.2 mol/L NaCl concentration.

(a)

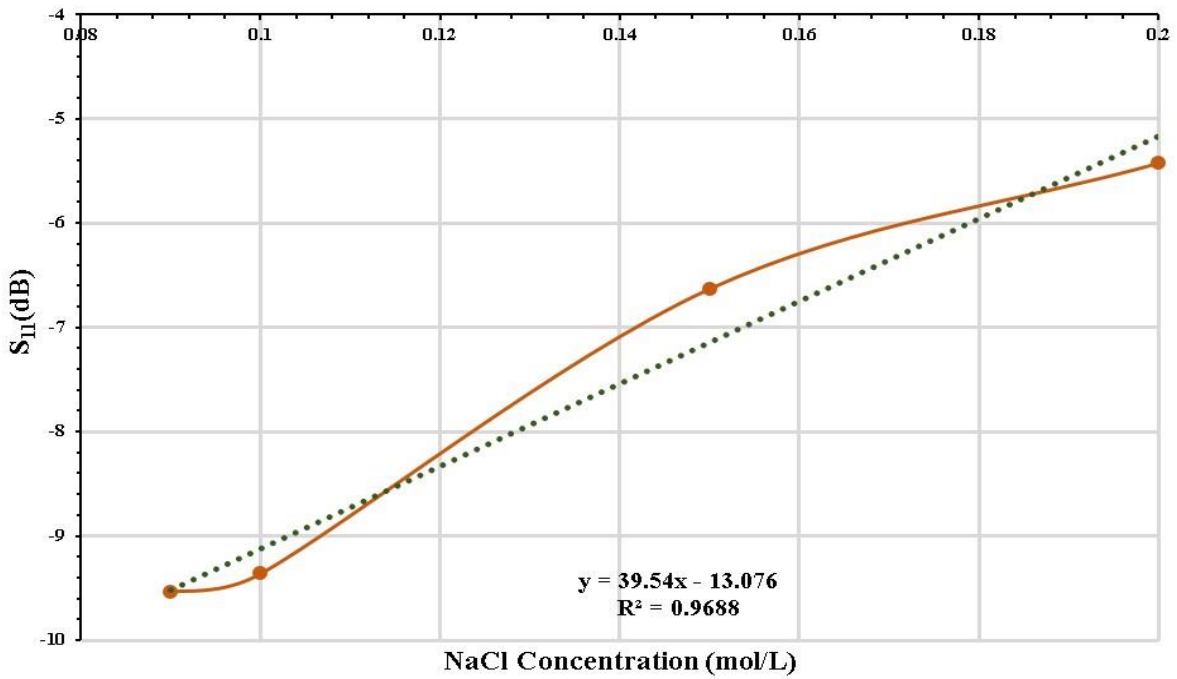


(b)

**Fig 4.22:**  $S_{11}$  Vs Concentration for 10% decrease antenna size by varying feedline (a) from 0.01 to 0.09 mol/L NaCl concentration (b) from 0.09 to 0.2 mol/L NaCl concentration.

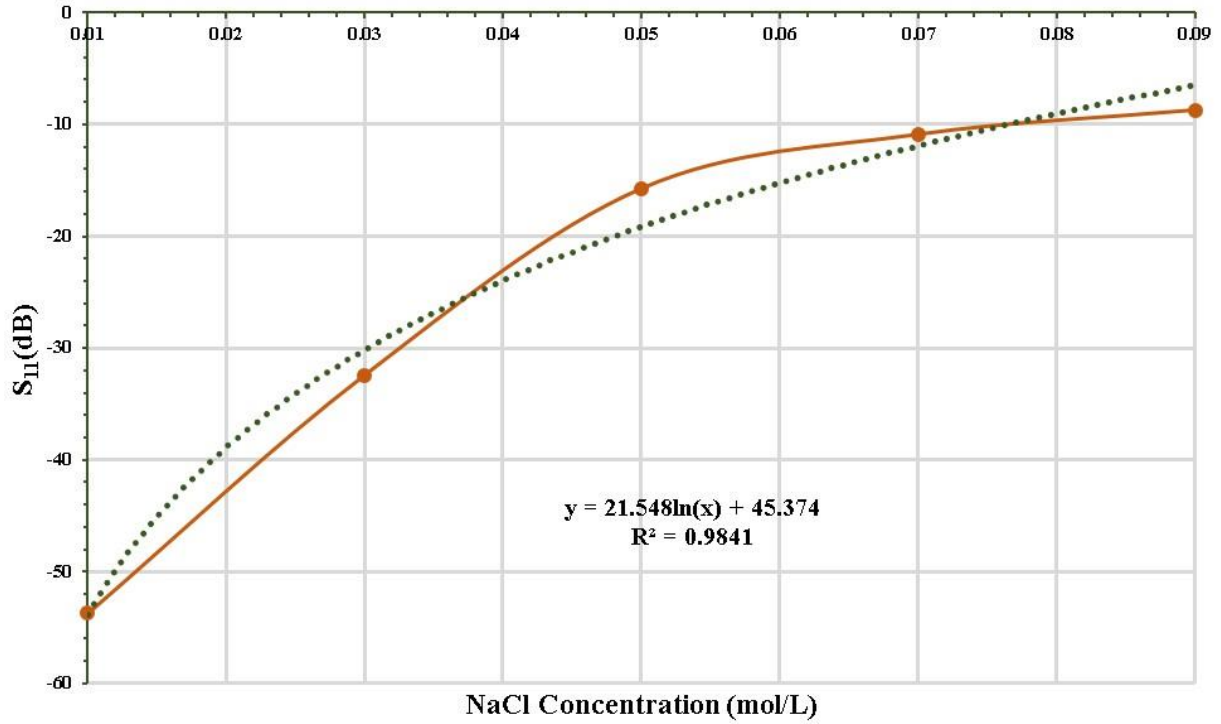


(a)

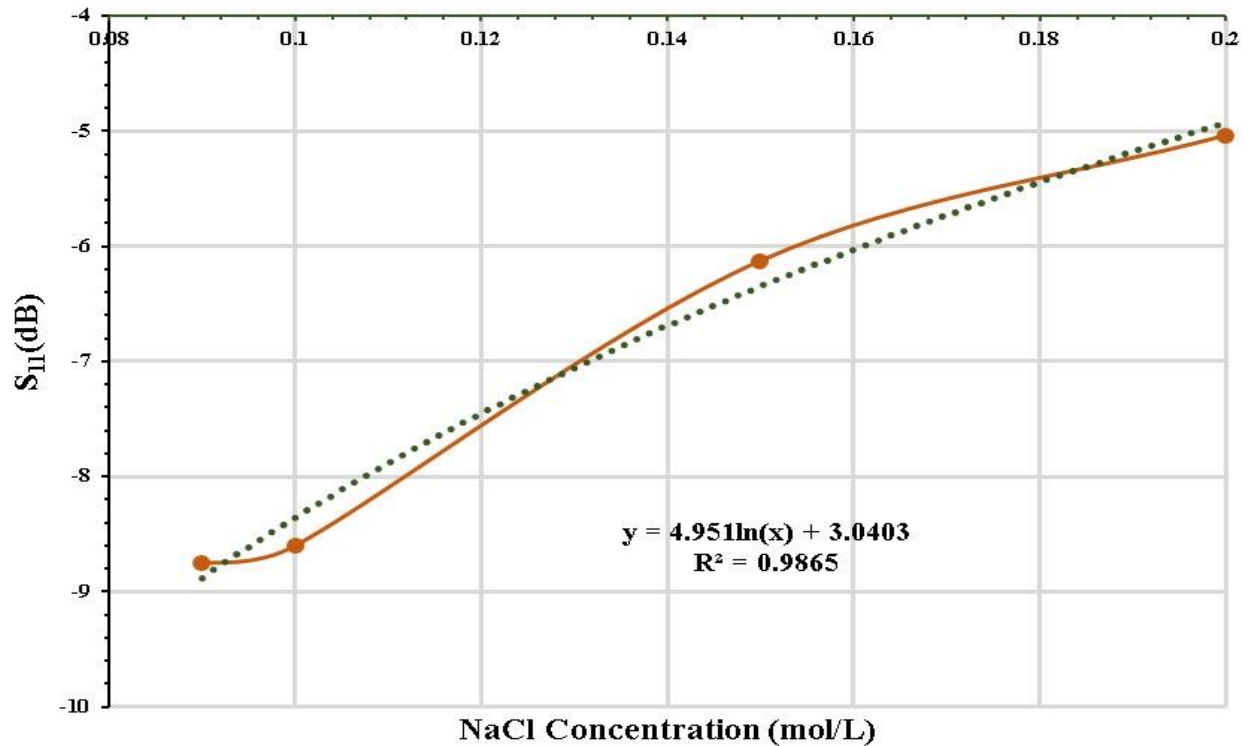


(b)

**Fig 4.23:**  $S_{11}$  Vs Concentration for actual antenna size by varying feedline (a) from 0.01 to 0.09 mol/L NaCl concentration (b) from 0.09 to 0.2 mol/L NaCl concentration.



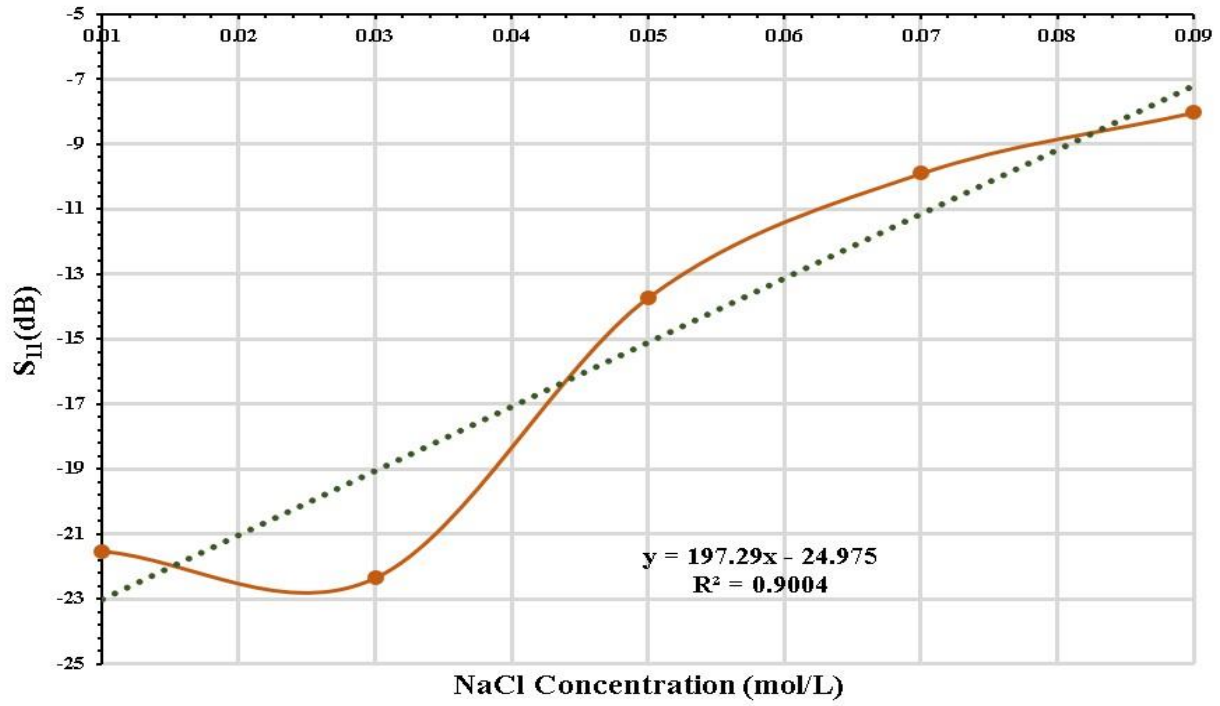
(a)



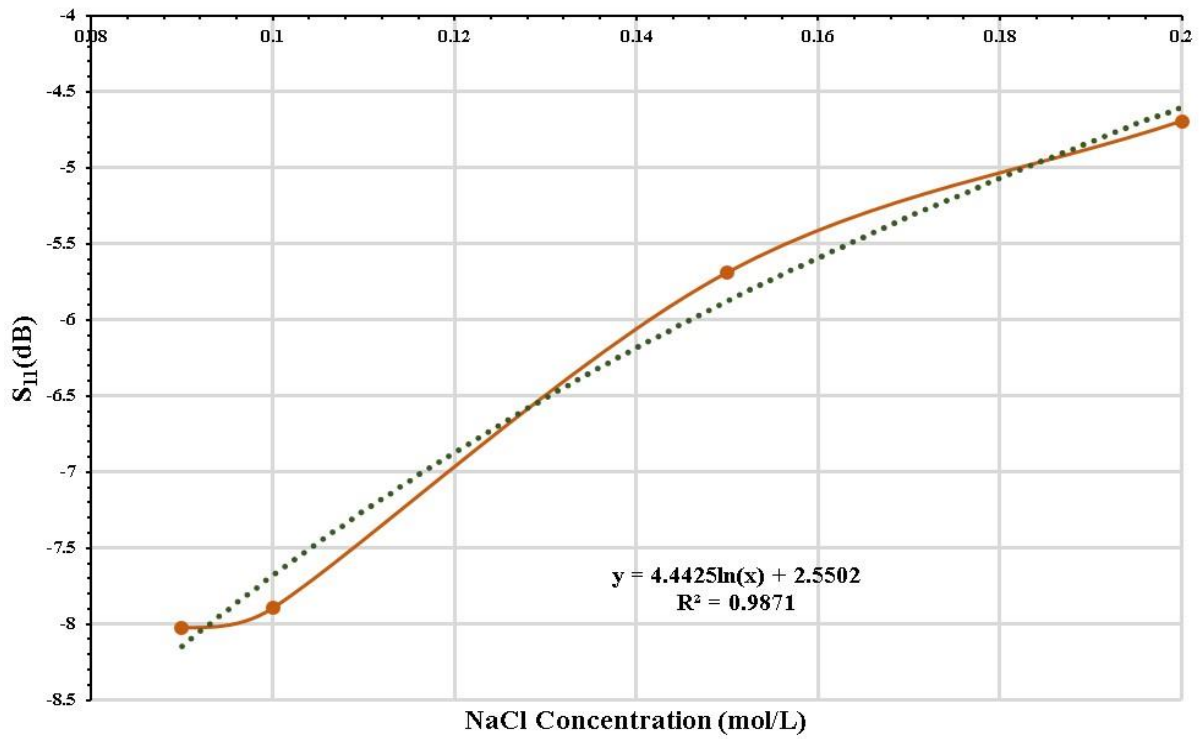


(b)

**Fig 4.24:**  $S_{11}$  Vs Concentration for 10% increase antenna size by varying feedline (a) from 0.01 to 0.09 mol/L NaCl concentration (b) from 0.09 to 0.2 mol/L NaCl concentration.



(a)



(b)

**Fig 4.25:**  $S_{11}$  Vs Concentration for 20% increase antenna size by varying feedline (a) from 0.01 to 0.09 mol/L NaCl concentration (b) from 0.09 to 0.2 mol/L NaCl concentration.

### 4.2.3 Error Calculation

Like before, from the software-driven results & equation-driven results there is a discrepancy. These errors can occur due to temperature changes because all the values of dielectric properties of NaCl solutions are taken based on room temperature. The following table will briefly show the errors for a particular concentration of NaCl solution.

Here we've taken 0.062 mol/L NaCl concentration as reference. The plot of  $S_{11}$  Vs Resonant frequency for five different MPA-based sensor sizes is also shown below.

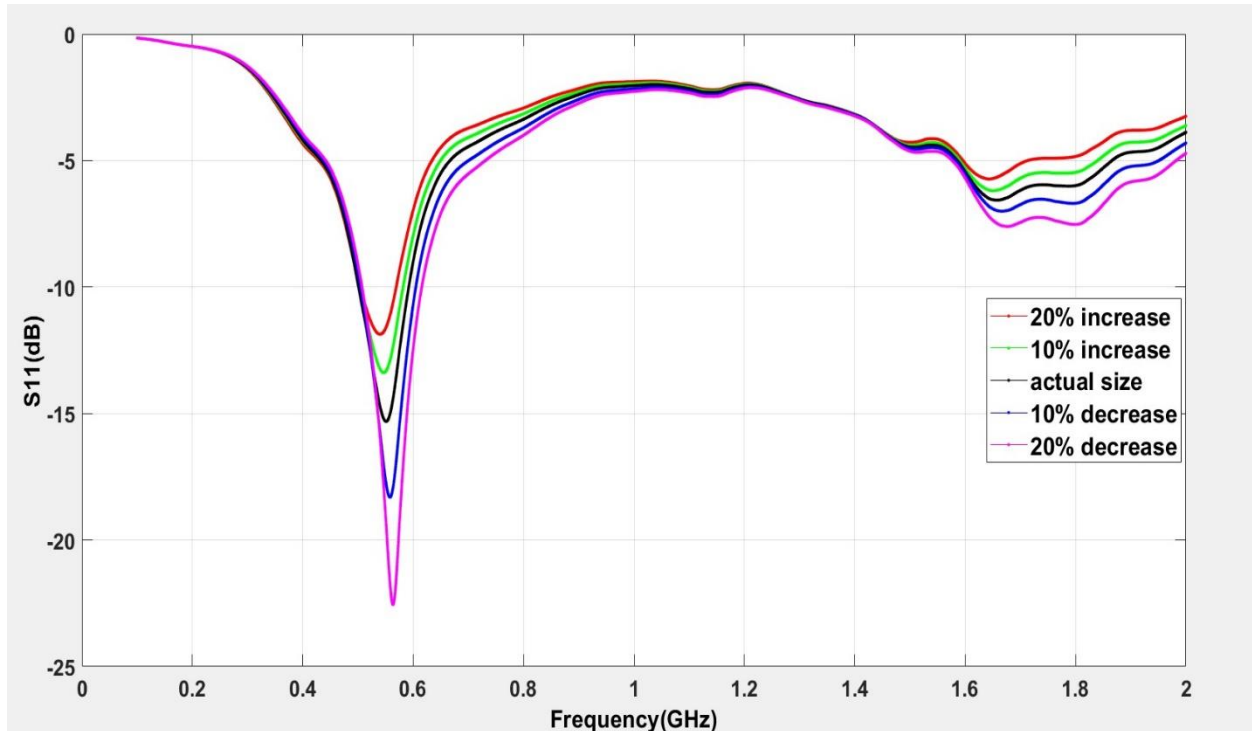


**Fig 4.26:**  $S_{11}$  Vs Resonant frequency plot for five different MPA-based sensor size by varying feedline and having NaCl Concentration 0.062 mol/L

**Table 4.4:** Error chart for 0.062 mol/L concentration of NaCl solution (Feedline width variation)

Antenna Size	Error percentage ( $S_{11}$ vs. conc)	Error percentage (Freq vs. conc)
20% decrease	2.33	0.56
10% decrease	5.15	0.39
Actual Size	1.94	0.177
10% increase	8.66	0.63
20% increase	7.38	2.66

### 4.3 Discussion

From the sensitivity chart we can see that for various sizes in terms of resonant frequency shift antenna with 20% decrease in dimensions give the highest sensitivity which is  $0.2409 \text{ GHzmol}^{-1}\text{L}$ . But when sensitivity is considered in terms of reflection coefficient ( $S_{11}$ ) the antenna with 10% increase in dimensions from the original size gives highest sensitivity which is  $161.696 \text{ dBmol}^{-1}\text{L}$ . For  $0.062 \text{ mol/L}$  concentration 20% increase shows least difference in between results obtained from COMSOL design and results obtained from equations for resonant frequency shift. Its value is 0.03%. For reflection coefficient ( $S_{11}$ ) 20% decrease shows the least value. Its value is 1.14%. For feed line width variation case 20% decrease will show highest sensitivity for resonant frequency shift. Its value is  $0.2513 \text{ GHzmol}^{-1}\text{L}$ . For reflection coefficient ( $S_{11}$ ) 10% increase shows the highest sensitivity which is  $121.625 \text{ dBmol}^{-1}\text{L}$ . For  $0.062 \text{ mol/L}$  actual size shows least difference between COMSOL design and results obtained from equations for both resonant frequency case and reflection coefficient case. Their values are 0.177% and 1.94% respectively. Total size variation shows higher sensitivity than feed line width variation for 10% and 20% increase when it comes to resonant frequency shift. For 10% and 20% decrease feed line width variation shows higher sensitivity. Feed line width variation shows higher sensitivity compared to total size variation for 10% and 20% decrease when it comes to reflection coefficient shift. For 10% and 20% increase total size variation shows higher sensitivity. When it comes to comparing errors resonant frequency shift shows better result than  $S_{11}$  for both total size variation and feed line width variation for all the cases. From the above points we see that we have to make a trade-off between sensitivity and error to get the best possible result as per our requirements. In cases where higher sensitivity is required we will use antenna sizes and parameters that gives highest sensitivity. Cases where precision is of utmost importance we will use antenna sizes and parameters that results in least error.

# Chapter 5

## Future goals and Conclusion

### 5.1 Introduction

For our thesis project, we undertook the task of building a micro-strip patch antenna-based sensor that can detect the electrolyte level in the human body from sweat. To do this we designed various antennas with different sizes and feed line widths. Then we compared these antennas for various parameters to see which of them works best for which purpose. The results showed that some specific size of antenna works best in some specific frequency range. Their sensitivities also vary substantially with different sizes and parameters. A lot of times sizes or parameters that show higher sensitivities will show higher errors. So antenna should be designed and used as per the users' requirements. The results of our research give an overall idea about what sizes and parameters work best in which scenario. This will not only help antenna manufacturers but also pave the way for future research to improve non-invasive electrolyte detection techniques.

### 5.2 Future goals

Our future goal is to compare the antenna sensitivity, linearity and error for different shapes. By varying the shape of the antenna we will understand how different shapes for patch, feed-line and stub affect its electromagnetic properties. We will then be able to build antennas for a wide variety of requirements. We also want to expand upon our already done experiment where we want to increase and decrease our total antenna size and feed line width size further. Testing our antenna for a wide range of sizes will help us compare their sensitivities, linearities and errors and build a pattern of how changing sizes results in changes in electromagnetic characteristics. Furthermore, we want to give physical shape to our designed antenna. To do this we will try to contact well-known antenna developing companies from home and abroad and have them manufacture the antennas with the required characteristics. At the end of the day, our ultimate goal is to make a low-cost means of electrolyte detection device that is fast and easy to use and will give accurate electrolyte measurements from the human sweat.

### 5.2 Conclusion

Nowadays as people are busier than ever there is a dire need for simple, portable and cheap sensor's that people can use on the go to measure various important body parameters. Electrolyte level is

one such parameter. Electrolyte imbalance in the human body will not only cause health hazards but also could be fatal in extreme cases. That's why it is of immense importance that we can find a simple, cheap, portable and cost friendly way of measuring electrolyte in human body. Our proposed micro-strip patch antenna will not only make this feasible but also provide ways for making changes to meet various requirements.

